Methods for automatized detection of rapid changes in lateral boundary condition fields for NWP limited area models

Martina Tudor

August 11, 2017

Contents

List of Tables

List of Figures

Chapter 1

Detection methods

Methods for automatized detection of rapid changes in lateral boundary condition fields for NWP limited area models

1.1 Abstract

Three hourly temporal resolution of lateral boundary data for limited area models (LAMs) can be too infrequent to resolve rapidly moving storms. This problem is expected to be worse with increasing horizontal resolution. In order to detect intensive disturbances in surface pressure moving rapidly through the model domain, a filtered surface pressure field (MCUF) is computed operationally in the ARPEGE global model of Météo France. The field is distributed in the coupling files along with conventional meteorological fields used for lateral boundary conditions (LBCs) for the operational forecast using limited area model ALADIN (Aire Limitée Adaptation dynamique Développement InterNational) in the Meteorological and hydrological service of Croatia (DHMZ). Here an analysis is performed of the MCUF field for the LACE coupling domain for the period since 23rd January 2006, when it became available, until 15th November 2014. The MCUF field is a good indicator of rapidly moving pressure disturbances (RMPDs). Its spatial and temporal distribution can be associated to the usual cyclone tracks and areas known to be supporting cyclogenesis. Alternative set of coupling files from IFS operational run in ECMWF is also available operationally in DHMZ with 3 hourly temporal resolution but the MCUF field is not available. Here, several methods are tested that detect RMPDs in surface pressure a posteriori from the IFS model fields provided in the coupling files. MCUF is computed by running ALADIN on the coupling files from IFS. The error function is computed using one time step integration of ALADIN on the

coupling files without initialization, initialized with digital filter initialization (DFI) or scale selective DFI (SSDFI). Finally, the amplitude of changes in the mean sea level pressure is computed from the fields in the coupling files. The results are compared to the MCUF field of ARPEGE and the results of same methods applied to the coupling files from ARPEGE. Most methods give a signal for the RMPDs, but DFI reduces the storms too much to be detected. The error function without filtering and amplitude have more noise, but the signal of a RMPD is also stronger. The methods are tested for NWP LAM ALADIN, but could be applied to other LAMs and benefit the performance of climate LAMs.

1.2 Introduction

Operational lateral boundary conditions (LBCs) are provided to limited area models (LAMs) at a time interval of several hours, refered to as the coupling update period. These data are used at lateral boundaries of the LAM domain every LAM time-step of several minutes. Consequently, LBC data of the large scale model are (linearly) interpolated in time. The interpolation procedure distorts the model fields and can lead to LAM forecast failures in case of fast propagating storms. The problem of linear interpolation of model fields in time for cases with rapidly moving storms that enter the LAM domain is expected to become worse as both global models and LAMs move to higher resolutions. These storms are associated to rapidly moving pressure disturbances that will be refered as RMPDs in this text. The problem could be even more pronounced in climate LAM's that couple to large scale data that are available with a longer interval.

One needs LBC data to represent scales that are too large to be periodic on LAM domain ([Laprise(2003)]). Various schemes for treating LBC data suffer from different problems ([Davies(1983)]). Model errors propagate from the lateral boundaries through the domain during the forecast time ([Nicolis(2007)]), these errors amplify and spread further with longer time of integration ([Nutter et al.(2004)]). A large LAM domain was recommended ([Staniforth(1997)]) to prevent boundary induced errors from propagating to the area of interest. However, there are problems that can not be cured by making LAM domain larger ([Vánnitsem and Chome (2005)]). For an overview of issues related to LBCs, see [Warner et al.(1997)].

Regional climate models are expected to develop small scale features due to high resolution surface forcings, nonlinearities in atmospheric dynamics and hydrodynamic instabilities ([Denis et al.(2002)]). Large coupling update interval can make LBCs act as a filter of small scale features that (should)

enter the LAM domain. Climate LAM without small scale information in the initial conditions and LBCs develop small scale variance even in the absence of surface forcing due to nonlinear cascade of variance ([Laprise(2008)]), but it takes several days.

Currently, there are two sets of LBC data that can be used for operational forecast using ALADIN ([ALADIN International Team(1997)]) (Aire Limitée Adaptation dynamique Développement InterNational) LAM in Meteorological and Hydrological Service of Croatia (DHMZ). One is from global Integrated Forecast System (IFS) of the European Centre for Medium-Range Weather Forecasts (ECMWF) and another is from the global model Action de Recherche Petite Echelle Grande Echelle (ARPEGE, see eg. [Cassou and Terray(2001)]) of Meteo France. The LBCs from the global numerical weather prediction (NWP) models ARPEGE and IFS are operationally provided with a 3 hour interval. These are used for running the operational ALADIN forecast in 8km resolution ([Tudor et al. (2013)]). Coupling is performed along the lateral boundaries in the 8 gridpoints from domain edge by means of [Davies(1976)] coupling scheme and using linear interpolation in time of the input fields from the global model.

[Termonia(2003)] has analysed the Lothar storm ([Wernli et al.(2002)]) and found that the three hourly coupling update interval is insufficient for resolving the storm in lateral boundaries. Also, [Davies(2014)] finds that 3 hourly LBCs lose information for 12km resolution LAM coupled to 12km resolution large scale model (see Figure 5c in [Davies(2014)]). In order to monitor the occurrence of potential LAM forecast failures due to insufficient coupling update frequency, a recursive high-pass filter ([Termonia(2004)]) has been implemented to the ARPEGE model and applied to the surface pressure field. The filtered surface pressure field is refered to as monitoring of the coupling update frequency (MCUF) field. Large values of the MCUF field indicate a RMPD in the surface pressure through that model grid point. A value larger than a threshold value suggests that a fast cyclone has moved through the area.

The MCUF field is provided since 06 UTC run on 23rd January 2006 in the coupling files from global model ARPEGE, run operationally in Meteo France, for the common coupling domain used for LBC data in 6 countries (Austria, Croatia, Czech Republic, Hungary, Slovakia and Slovenia). This common domain will be refered to as the LACE domain (Limited Area for Central Europe). The horizontal resolution of the LACE coupling domain provided from ARPEGE has changed over the years (see Table 1.1) but the aerial coverage of the LACE coupling domain provided from ARPEGE remained te same (see the aerial coverage of the green isolines in Figure 1.1). Local operational domains are smaller than the LACE domain, but

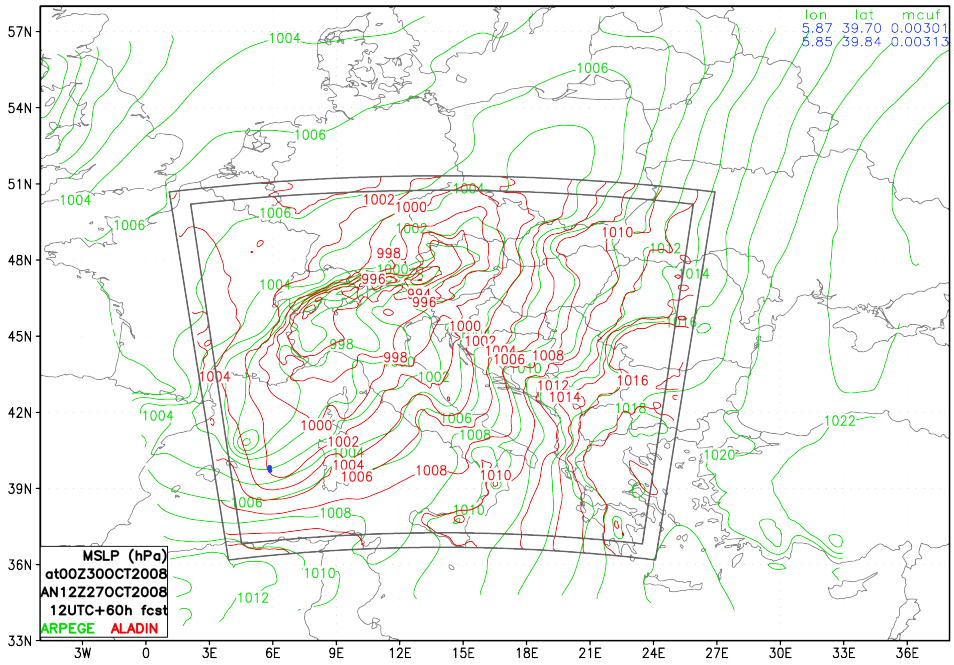

Figure 1.1: Mean sea level pressure (hPa)from ARPEGE (green) and ALADIN (red) operational 60 hour forecast starting from 12 UTC analysis on 27^{th} Oct 2008. The coordinates and values of MCUF field exceeding the 0.003 threshold are listed in the upper right corner and plotted as blue dots on the map.

have higher horizontal resolution and have coupling zones 8 gridpoints wide along lateral boundaries. If the point with the large MCUF value is inside the coupling zone of the ALADIN domain, it can be expected that the ALADIN model run will miss the cyclone strength due interpolation of boundary data in time. These events are expected to be rare, at least according to the analysis performed on one year of data for the Belgian domain ([Termonia et al.(2009)]). But rapid changes in surface pressure are associated to the most intensive storms moving rapidly, pose a threat to the public and require warning. It is very important that operational NWP models forecast such events. The frequency of such events is analysed for the LACE domain on almost 9 years of data from the operational ARPEGE fields (since 23rd January 2006 until 15th November 2014).

Table 1.1: Model (ARP-ARPEGE), period (form 06 UTC on first date to 00 UTC on the last date), horizontal resolution and total number of the coupling files for which the rapid changes of surface pressure field were analyzed, the field was used received from Meteo-France and computed by ALADIN for files received from ECMWF. The rapid changes in surface pressure for the first 3 hours were ommited from the analysis due to evidence of model spin-up for some periods.

model	period (from-to)	resolution (km)	total num of files	whole > 0.003	domain > 0.004	MCUF > 0.005	> 0.003 cpl zone
ARP	23Jan2006 – 06Feb2008	20.678	64292	906	270	93	235
ARP	06Feb2008 – 11May2010	15.400	72600	1017	383	141	400
ARP	11May2010 – 16Nov2014	10.610	151756	1122	293	125	243
ARP	23Jan2006 – 16Nov2014	all	288648	3045	946	359	878
ARP	01Nov2010 – 16Nov2014	10.610	129674	995	259	108	186
IFS	01Nov2010 – 16Nov2014	15.400	147350	698	178	67	109

The most obvious solution to this problem is to increase the frequency of the available LBC data and most of the centres that run both global models and LAMs use hourly input fields for the LAMs. However, this solution is not very practical for the meteorological services that run only LAMs and rely on LBC data from somewhere else. On the other hand, if 3 hourly data is insufficient for global model run in roughly 16 km resolution and LAM in 8 km resolution, then hourly data would be less satisfactory when both global model and LAM move to higher resolutions (as was already announced at various meetings in 2014). Also, running old cases from stored archive data requires using LBCs with 3 hours interval.

There are other solutions proposed to solve the problem of errors in LBCs caused by time interpolation of fields. The first one ([Termonia et al.(2009)]) is to restart the model forecast from the coupling file when the storm is inside the domain using the scale selective digital filter initialization ([Termonia(2008)]). The second one is to insert the storm by means of gridpoint nudging ([Termonia et al.(2011)]). Both of these require to stop the model run, insert the storm artifically and continue the model run from there. Using corrected interpolation with time derivatives ([Termonia(2003)]), Boyd's periodization method ([Boyd(2005), Termonia et al.(2012)]) can also improve the forecast ([Degrauwe et al.(2012)]), and alternative methods of interpolating LBC data in time ([Tudor and Termonia(2010)]) do not require restarts, but are computationally expensive, so these would also be used only when needed. However, in order to apply any of these solutions, we should first detect the RMPD in the fields used on lateral boundaries.

Using MCUF implies that the global model computes it operationally and distributes the field in the output files together with the other forecast fields. However, LAM can be coupled to various global model forecasts or larger scale LAMs for operational forecast, and re-analyses for climate model studies or simulations of specific phenomena. With the exception of ARPEGE, global models do not provide a field that would diagnose rapid changes in pressure that occured in each grid-point during a time interval between two consecutive output files. The centers that provide global model fields could be discouraged to compute MCUF field due to computational cost and potentially complex implementation in the model code, and especially to re-run the re-analysis cycles to provide such data for studies of historical weather. It is therefore usefull to detect RMPDs a posteriori using the standard meteorological fields usually provided in model output. The method should enable automatic detection of a RMPD to be usefull in the operational forecast as well as in the climate simulations using LAM. As pointed by the reviewers, fast-moving disturbances in the upper layers of the atmosphere or inertia-gravity waves are more common. These are also a source of error in LAMs while MCUF detects disturbances in the surface pressure. The focus of this article are rapidly moving disturbances in surface pressure, but a method that detects them could be applied to an upper level field.

LAMs used for simulations of climate use input LBCs that are available in coupling update interval of 3 hours or more. Simultaneously, LAMs tend towards higher horizontal resolutions. A number of climate studies has been performed ([Horvath et al.(2011), Hamdi et al.(2012), De Troch et al.(2013), Hamdi et al.(2014)]) using ALADIN in combination with ERA40 ([Uppala et al.(2005)]) and ERAInterim ([Dee et al.(2011)]) datasets for LBCs. These applications would also benefit from a method that would detect RMPDs a-posteriori from the standard meteorological fields used for LBC.

The NWP suite at DHMZ is focused on forecasting weather on the area of Croatia. Cyclones that affect that area often originate from western Mediterranean and Adriatic ([Horvath et al.(2008), Horvath et al.(2009)]) that is recognized as a particularly active region with respect to cyclones ([Campinis at al.(2000), Alpert et al.(1990)]). Severe precipitation events occur when cyclone produces convergence of the moist air and a large quantity of precipitable water ([Lionello et al.(2006)]). Western Mediterranean experiences flash flood events that arise from extremely high rainfall rates ([Doswell et al.(1996)]).

The MCUF field is not provided in the LBC files of IFS provided by ECMWF. On 1st January 2014 the operational ALADIN forecast in DHMZ has switched to using IFS coupling files. It is possible to compute MCUF field by running ALADIN on the resolution and domain of the coupling fields. Here an analysis is performed of the MCUF field computed by running AL-

ADIN for the common LACE coupling domain for the files provided from IFS since 27th October 2010 until 15th November 2014. Otherwise, it is possible to estimate the error that arises due to linear interpolation of LBC data in time ([Termonia(2003)]) from model tendencies obtained by running ALADIN for one time step. The error was estimated for surface pressure and mean sea level pressure using coupling data without initialization, or initialized to remove the high frequency noise. Additionally, this work proposes to estimate the magnitude of pressure variations by computing a simple amplitude of oscillations between the successive coupling files.

The next section describes the models briefly, the methods used to detect RMPDs and the effect of linear interpolation in time on mean sea level pressure. The analysis of 9 years of the MCUF field from ARPEGE is presented in Section 3. Results of methods for detecting RMPDs in IFS coupling fields are presented in Section 4. The last section gives conclusions.

1.3 Model description and metods of detection of rapidly moving pressure disturbances

1.3.1 Operational forecast model

ALADIN is used for operational weather forecast in DHMZ in 8 km resolution using hydrostatic dynamics, 2-time-level semi-implicit semi-Lagrangian and stable extrapolation two-time-level scheme ([Hortal(2002)]). Operationally, the model uses 37 levels in the vertical and a mass-based hybrid terrain-following vertical coordinate η ([Simmons and Burridge (1981)]).

The initial conditions for the operational forecast are obtained using data assimilation procedure ([Stanešić(2011)]). Details of the operational forecast suite as well as model set-up are provided in [Tudor et al. (2013)]), but there were few changes. The forecast is run up to 72 hours four times a day, starting from 00, 06, 12 and 18 UTC analyses, and coupled to LBC fields from IFS in delayed mode. This means that LBC for 6 hour forecast from 18 UTC run of IFS is used for initial LBC for 00 run of the next day, 9 hour forecast from 18 UTC run of IFS is used for 3 hour forecast LBC for 00 run of the next day, and so on.

The 8km resolution operational forecast is coupled to a global model on the 8 points wide zone alnog lateral boundaries using relaxation tecnique ([Davies(1976)]) and linear interpolation of LBC data in time ([Haugen and Machenhauer(1993), Rádnoti (1995)]). Each coupling file contains the complete set of fields

needed to initialize the ALADIN model forecast.

Digital filter initialization (DFI) is implemented in ALADIN in order to remove high-frequency noise ([Lynch and Huang(1992)]) that arise due to interpolation of the coupling fields from the global model grid to the grid of the coupling files and then again to the resolution of the LAM (and changes in height of topography in different models/resolutions). Since DFI can considerably reduce the depth of the RMPD due to the Doppler effect, alternative scale selective digital filter initialization (SSDFI) was proposed, implemented and tested in the ALADIN model ([Termonia(2008)]).

1.3.2 Global model ARPEGE

)

ARPEGE is a global sem-lagrangian spectral model run operationally at Meteo France on a stretched and rotated grid ([Courtier and Geleyn(1988)]) with highest horizontal resolution over France and lowest resolution on the opposite side of the Earth. The horizontal resolutions in the model forecast and data assimilation procedure were changing during the 9 years when the MCUF field was computed in the operational ARPEGE forecast. The horizontal resolution of the coupling files also changed twice, see Table 1.1.

ARPEGE can use coarser resolution in variational data assimilation procedure than in the forecast run. The fields from the operational forecast are interpolated from the stretched and rotated native model grid to the grid of the limited area LACE domain in Lambert projection of the coupling files.

The fields from operational ARPEGE forecasts are available in the coupling files with 3 hour interval for 4 runs per day (starting from 00, 06, 12 and 18 UTC analyses) and extending up to 72 for the 00, 06 and 12 UTC runs and up to 60 hours for the 18 UTC run. ARPEGE computes the MCUF field operationally according to [Termonia(2004)] and the field is distributed in the coupling files.

1.3.3 Global model IFS

IFS is also a global spectral model that uses semi-Lagrangian advection. It is run oparationally at ECMWF with uniform horizontal resolution over the globe. The details of the operational set-up in the model forecast and data assimilation have changed over the years used for this study, while the LBC files were available operationally, as did the operational model versions. The model forecast fields are interpolated from the IFS model grid to the LAM grid in Lambert projection and the horizontal resolution of the coupling files remained 15.4 km (see Table 1.1).

Following the research studies where LBC data from IFS has been used for studies of severe weather cases ([Ivatek-Šahdan and Ivančan-Picek(2006), Branković et al.(2007), Branković et al.(2008)]), the operational forecast run of the ALADIN model in DHMZ has switched to uding LBC data from IFS on 1st January 2014.

The MCUF field is not computed by the IFS operational suite and therefore not available in the coupling files from IFS provided by ECMWF. Rapid changes in the surface pressure or the mean sea level pressure were detected in the fields provided from IFS operational forecast in the coupling files on the LACE common domain using a number of tools.

- ALADIN was run on the LACE domain (in the resolution of the coupling files) with 600 seconds time step and the MCUF field was computed during the model run. The computed MCUF field will be referred to as IFSM. However, this means that a different model was run (different dynamics and physics) and the results can be different than when computed in the host model.
- The error function from [Termonia(2003)] was computed by running one time-step forecast starting from fields in the coupling files (in the same horizontal and vertical resolution), three sets of experiments were performed using initialization without filtering, using DFI or SSDFI.
- The amplitude of the oscillations in the surface pressure (and mean sea level pressure) was computed from three consecutive coupling files.

The last item actually detects situations when the moving pressure disturbance would be missed using $2\Delta t$ (6 hours) coupling update interval not the Δt (3 hours) interval. But the large values of this field can mean that the interval as short as Δt can also be insufficient for proper representation of lateral boundary data by linear interpolation of the LBC fields in time.

1.3.4 Computing the monitoring of the coupling update frequency (MCUF) field from the ECMWF coupling files

ALADIN can compute the MCUF field during the model forecast. The field was computed by running ALADIN on the LACE domain of LBC files from operational IFS with horizontal resolution of 15.4 km (the same resolution and grid as the coupling files) and a time-step of 600 seconds. The output IFSM field is written with 3 hourly interval. The same procedure has been

performed on the LBC files provided since 27th October 2010 until 15th November 2014, for 4 runs per day (starting from 00, 06, 12 and 18 UTC analyses) and extending to 78 hours forecast.

The maximum value of the IFSM field on the domain covered by the coupling files has been computed for each forecast output file. The average IFSM has been computed, the number of files when it exceeded the critical value and the maximum value achieved in each grid point for the coupling files for 6 hours forecast and longer.

The same procedure applied to the ARPEGE coupling files

MCUF was also computed by running ALADIN on the domain and resolution of the coupling files from ARPEGE and this fileld is refered to as the ARPM field to distinguish it from the MCUF field computed in ARPEGE forecast. But the coupling files from the ARPEGE global model are provided in different horizontal resolutions that the files from IFS. There was no period when both coupling files used the same horizontal resolution (Table 1.1). It is more important to test the method on both sets of coupling files on the same period in time since the frequency of the occurence of the fast storms can have significant seasonal and annual variability.

1.3.5 The error function

Each coupling file contains the complete set of model fields that can be also used as a initial file to perform a forecast run using ALADIN model. The coupling data are used as initial fields to perform a model integration of one time step forward in time in order to obtain $F(t + \delta t)$ and the tendencies of the model variables. In order to avoid spurious high frequency noise, a filter initialization should be applied before the start of the model run.

When investigating the error due to linear interpolation of surface pressure, [Termonia(2003)] computes an error function from the surface pressure field and finds that its maximum over the model domain is a good indicator of a RMPD. Each coupling file contains the complete set of fields needed to initialize the model, so they can be used as initial fields to perform one time step model integration. [Termonia(2003)] defines a dimensionless estimate of the truncation error due to linear interpolation in time as

$$e_T = \frac{1}{4}\left|\frac{(F'(t_2) - F'(t_1))\,(t_2 - t_1)}{F(t_1) + F(t_2)}\right|. \tag{1.1}$$

Where $F(t_{1,2})$ are the values of the model field F at times when the LBC data are available in the coupling files and $t_2 - t_1$ is therefore the coupling

update interval (3 hours). $F'(t_{1,2})$ is the tendency of the field F at time $t_{1,2}$ and can be computed as $F'(t_{1,2}) = \frac{F(t_{1,2}+\delta t)-F(t_{1,2})}{\delta t}$ where δt is the model time step. The error function of surface pressure and mean sea level pressure was computed for each coupling file. The tendencies can be computed without any filtering of the field in coupling files, using DFI ([Lynch et al.(1997)]) or SSDFI ([Termonia(2008)]).

The error function e_T has been computed for the surface pressure field from IFS coupling files. The maximum values over the model domain are

$$E_T = max(e_T(x, y)) \tag{1.2}$$

where e_T is the error computed in each grid point.

The error estimate E_T revealed cases when linear interpolation of the coupling data in time with 3 hour coupling update interval is insufficient for the Belgian domain ([Termonia(2003)]. Both E_T computed with or without filtering over the Belgian domain yield a clear signal when there is a intensive RMPD. But the domain of Aladin Belgium used in that work did not contain any strong orography. The Croatian domain (and hence the LACE coupling domain) contains mountains of considerable height (Alps, Apennines etc.).

Digital filter initialization

Coupling files contain already interpolated data (to a lambert conformal grid), not the data from the native global model grid. Horizontal interpolation of the surface pressure field (and other forecast fields) from native IFS grid and topography to the grid and topography of the LBC files also distorts the fields, so there could be spin-up when computing the tendencies. This change in geometry can generate high frequency noise that can be removed using DFI ([Lynch and Huang(1992)]). The DFI was applied using Dolph-Chebyshev filter on 14 time steps adiabatic backward integration and 14 time steps forward integration with a time step of 600 seconds. The time span was 2.333 hours, the stop band edge period was 3 hours, the ripple ratio 0.05 yields minimum time span of 2.07 hours ([Lynch(1997)]) used with the scheme for diabatic DFI in ALADIN ([Lynch et al.(1997)]).

Scale selective digital filter initialization

Doppler effect can shift the frequencies of RMPDs into the range of spurious gravity waves that DFI was designed to remove. Consequently, DFI reduces the intensity of RMPDs ([Termonia(2008)]). Alternative SSDFI is expected to be a better solution for initialize the fields used to compute the error function intended to detect RMPDs.

The SSDFI was applied using Dolph-Chebyshev filter on 8 time steps adiabatic backward integration and 8 time steps forward integration with a time step of 600 seconds. The time span was 1.333 hours, the stop band edge period was 1.5 hours, the ripple ratio 0.05 yields minimum time span of 1.019 hours and the cutoff frequency increases with wave number for 30 m/s ([Termonia(2008)]). This shorter time span and stop band edge period yields less filtering that preserves the storm in [Termonia(2008)] while still removing the spurious inertia gravity waves generated above mountains. Shorter time span means shorter model run which is also beneficial in the operational context.

Both filtering methods require running the model adiabaticaly backwards for a number of time-steps and then diabatically forward for the same number of time steps for each of the coupling files. The method is therefore computationally expensive if DFI or SSDFI are applied before computing the tendencies (about as expensive as IFSM).

1.3.6 The amplitude in the pressure variations

All the methods described previously require that all the coupling files (initial and forecast) contain the data necessary to initialize the LAM and run the LAM at least for one time step. Here a very simple method for detecting RMPDs is presented that does not require running LAM.

As a measure of variability in the model field, the following can be computed:

$$A = \frac{1}{2}\left(F(t_1) + F(t_3) - 2F(t_2)\right) \tag{1.3}$$

where $F(t_1)$, $F(t_2)$ and $F(t_3)$ are the values of the model field F at three consecutive times t_1, t_2 and t_3 when the coupling data are available. The differences in times is the coupling update interval $t_2 - t_1 = t_3 - t_2 = \Delta t$ which is operationally equal to 3 hours.

Eq.1.3 describes the changes of the model field F during the $2\Delta t$ period, eg. twice the coupling update period. Therefore, the values of A are largest in points where Δt period is actually enough to describe the evolution of the model variable during the coupling update interval using linear interpolation in time (eg. at the position of the pressure minimum at time t_2). However, A can be used as an indicator of a RMPD, as will be shown in the results of this study. On the other hand, A could miss the evolution of the model variable on a time scale less than Δt, for example when the model variable evolves as the full line in Fig 1 of Termonia (2003).

1.3.7 The effect of linear interpolation

An atmospheric disturbance can enter the domain unnoticed by the coupling scheme. The Figure 1.1 shows mean sea level pressure from the ARPEGE forecast (as provided in the coupling file) and mean sea level pressure from the ALADIN 8km forecast coupled to it.

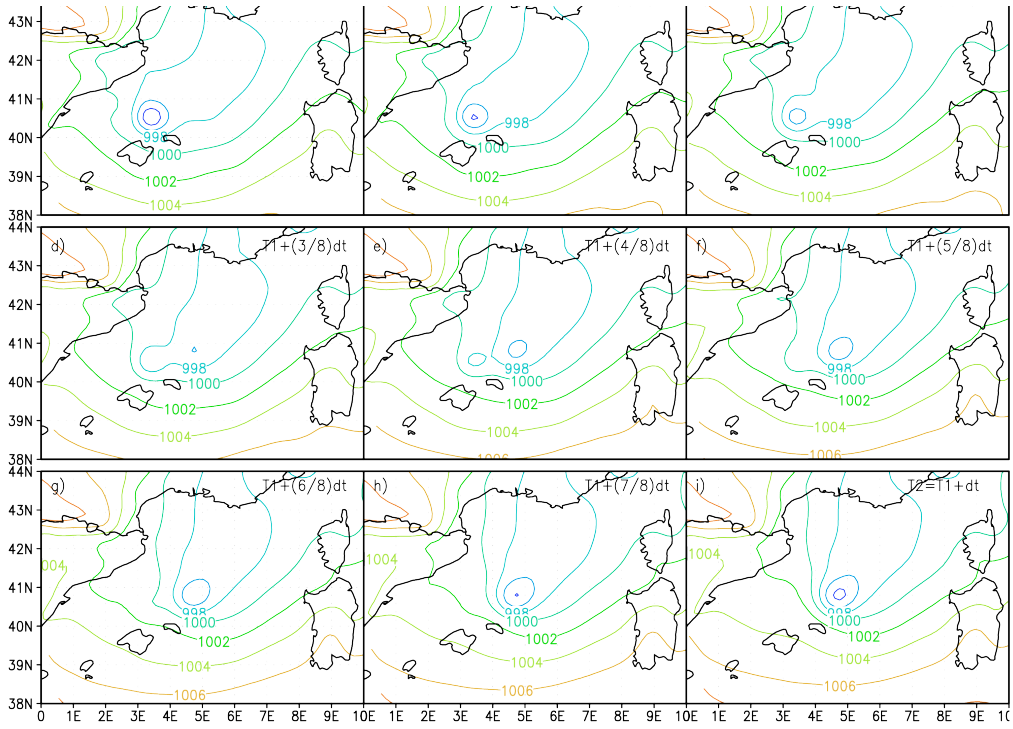

Figure 1.2: Mean sea level pressure (hPa) from ARPEGE operational coupling files starting from 12 UTC analysis on 27^{th} Oct 2008, 57 (a) and 60 (i) hour forecasts, linear interpolation of mean sea level pressure in time to half of the 3 hour coupling period (e), 1/8 of 3h (b), 1/4 (c) 3/8 (d), 5/8 (f), 3/4 (g) and 7/8 (h).

Linear interpolation in time distorts the model fields. Figure 1.2 shows the effect of linear interpolation on the mean sea level pressure. The ARPEGE forecast mean sea level pressure from two consecutive coupling files is interpolated linearly in time (as in the operational coupling procedure). In the place of moving storm, LAM sees a dual cyclone structure, one cyclone/storm disappears and another appears. This is why larger coupling zone yields dual cyclone structure, as was shown by [Tudor and Termonia(2010)].

Other meteorological fields that are used for coupling at lateral boundaries get distorted by linear interpolation in time if they contain high resolution features such as storms or meteorological fronts. For simplicity, this article will focus on the mean sea level pressure and surface pressure fields.

1.4 Filtered surface pressure field from ARPEGE

1.4.1 The time series of MCUF maxima

The maximum value of the MCUF field as computed in the operational ARPEGE has been extracted from each forecast coupling file available for the whole LACE coupling domain. The time series of MCUF maxima are shown in Figure 1.3. The MCUF maxima from the 3 hour forecast files were omitted in the plot since they had high values due to other phenomena that arose during spin-up following ARPEGE initialization, especially in the period until 6th February 2008. Most of the points with large MCUF values in the 3 hour ARPEGE forecast are close to mountains. This suggests large spin-up of the surface pressure field in the beginning of the ARPEGE forecast. Since these large values of MCUF in the +03 hour forecast mostly do not represent a storm that moves quickly through the domain, analysis has been performed only on fields from +06 hour forecast or larger.

MCUF exceeds the 0.003 value rather often, mostly in events that last a few days, up to a week. For each file where MCUF was larger than this threshold value, a figure was plotted with mean sea level pressure from the coupling file (ARPEGE) and the operational ALADIN forecast in 8 km resolution coupled to it, and the points where MCUF was larger than 0.003 (see example in Figure 1.1). Each time, large MCUF values were associated to a pressure disturbance in ARPEGE that was often less intensive in ALADIN forecast (if covered by the operational ALADIN domain).

The events that yield large values of the MCUF field represent RMPDs that rapidly traverse any part of the LACE domain. These events are more frequent in autumn, but appear throughout the year, least often during summer months. Several large MCUF values can be associated to a single event (one cyclone moving rapidly over the model domain), but they represent maxima from different forecast coupling files and different forecast runs (starting from different initial times corresponding to different ARPEGE analyses). On the whole LACE domain, the critical value of 0.003 has been exceeded 3045 times in 288648 files, more than 1% of the files in the whole period from 23rd January 2006 until 16th November 2014 (see Table 1.1). In 878 files, large MCUF values were close to the coupling zone of the operational

ALADIN domain in DHMZ (see Figure 1.1). This is only 0.3% of the coupling files and the event can be considered rare. But, as mentioned earlier, these events are perhaps most important to be forecast. In order to properly forecast such events using LAM, one should first detect it and then apply boundary error restarts ([Termonia et al.(2009)]) or gridpoint nudging ([Termonia et al.(2011)]).

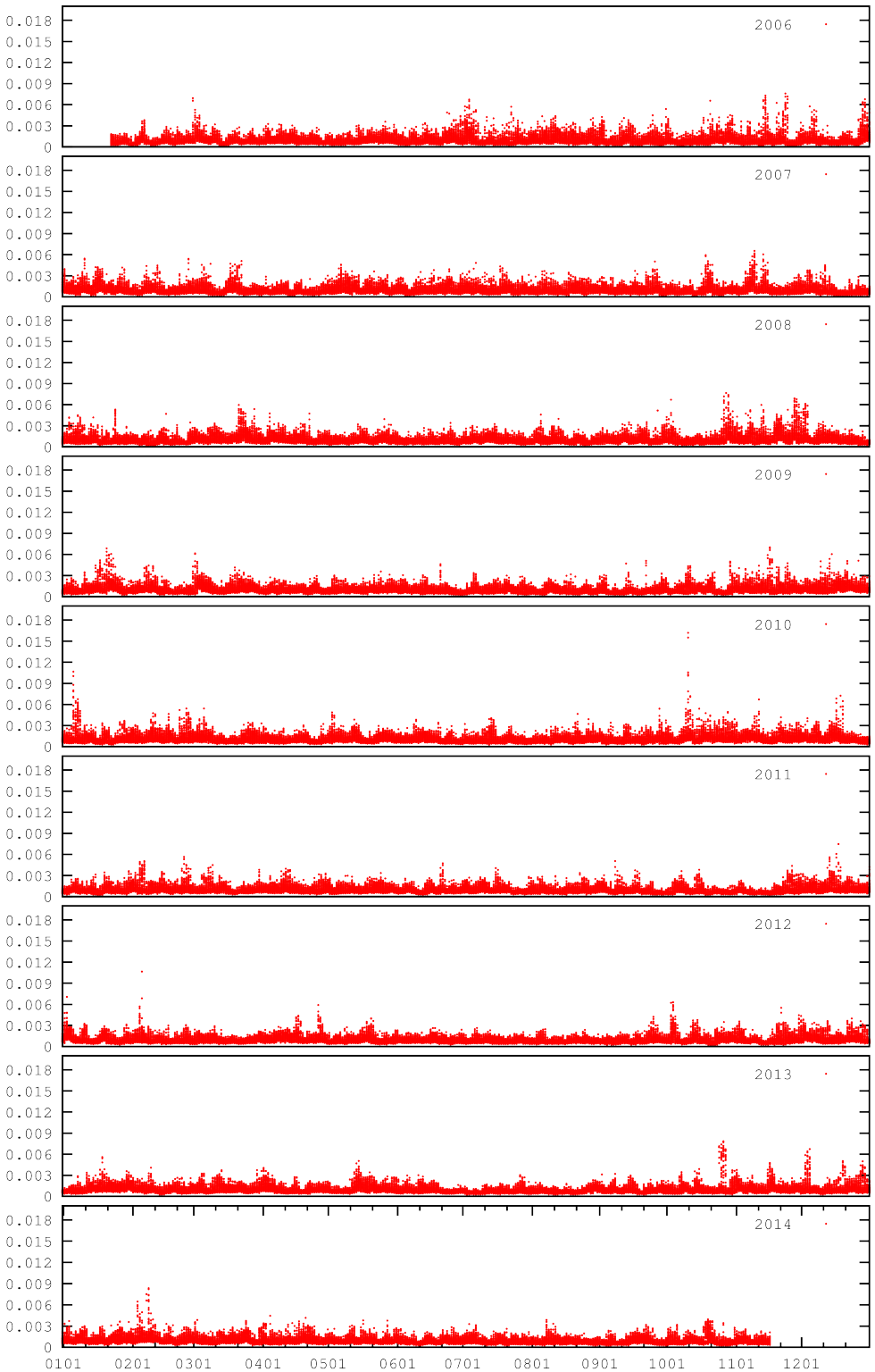

Figure 1.3: Maximum value of the MCUF field (units hPa) on the LACE coupling domain, provided from ARPEGE, from the coupling files for 6 hour forecast up to 72 hours forecast (60 hours for 18 UTC run), starting from 00, 06, 12 and 18 UTC analyses, since 23rd January 2006 until 15th November 2014.

1.4.2 Spatial distribution of MCUF from ARPEGE

Successfull implementation of the computations of the MCUF field in the operational ARPEGE means that it is not dependent on the horizontal resolution of the global model since ARPEGE is run on a stretched grid. The averaged MCUF fields (Figure 1.4) for different horizontal resolutions (Figure 1.4a for 20.678km, Figure 1.4b for 15.4 km and Figure 1.4c for 10.51 km) show that it does not depend on the resolution of the coupling files as well as the resolution of the global model where it was computed. Averaged MCUF field is slightly larger over the North Sea in the first period (from 23rd January 2006 until 6th February 2008) for the lowest resolution. The values over the Mediterranean have the highest values in the middle period (from 6th February 2008 until 11th May 2010) for the 15.4 km resolution of the coupling files. This result suggests that the cyclones traversed Mediterranean more often and faster during that period than in the periods before and after.

The maps of number of cases when the MCUF field exceeded the 0.003 threshold (Figure 1.5) show that the number of cases with fast cyclones over the North Sea is the largest in the last period (that is also twice as long as the other two). But over the Mediterranean, MCUF exceeded the critical value most often in the second period, as well as over the area under the influence of the Bay of Biscay.

The absolute maximum values of the MCUF field have large values over most of the western Mediterranean during the second period (Figure 1.6). The overall largest values of MCUF were computed during the third period (and in the highest spatial resolution) close to the coastline of Algeria, but the values are low over the rest of the Mediterranean. On the other hand, the maxima are the highest over the North sea in the last period and over the Black Sea in the first period.

The spatial distribution of the frequency of the events when MCUF exceeded the critical value (Figure 1.5) indicate which areas should be avoided as parts of the coupling zone if one wants to have fewer problems with properly resolving the boundary data in time with 3 hourly coupling update period. When the filtered surface pressure field is larger than a threshold value 0.003, there is a storm rapidly propagating through the area. If the point with the large value is inside the coupling zone of a LAM, it can be expected that the LAM forecast will miss the storm due to time interpolation of boundary data. The analysis of the MCUF field from ARPEGE coupling files for the common LACE coupling domain shows that this field is above the threshold far more frequently than acceptable.

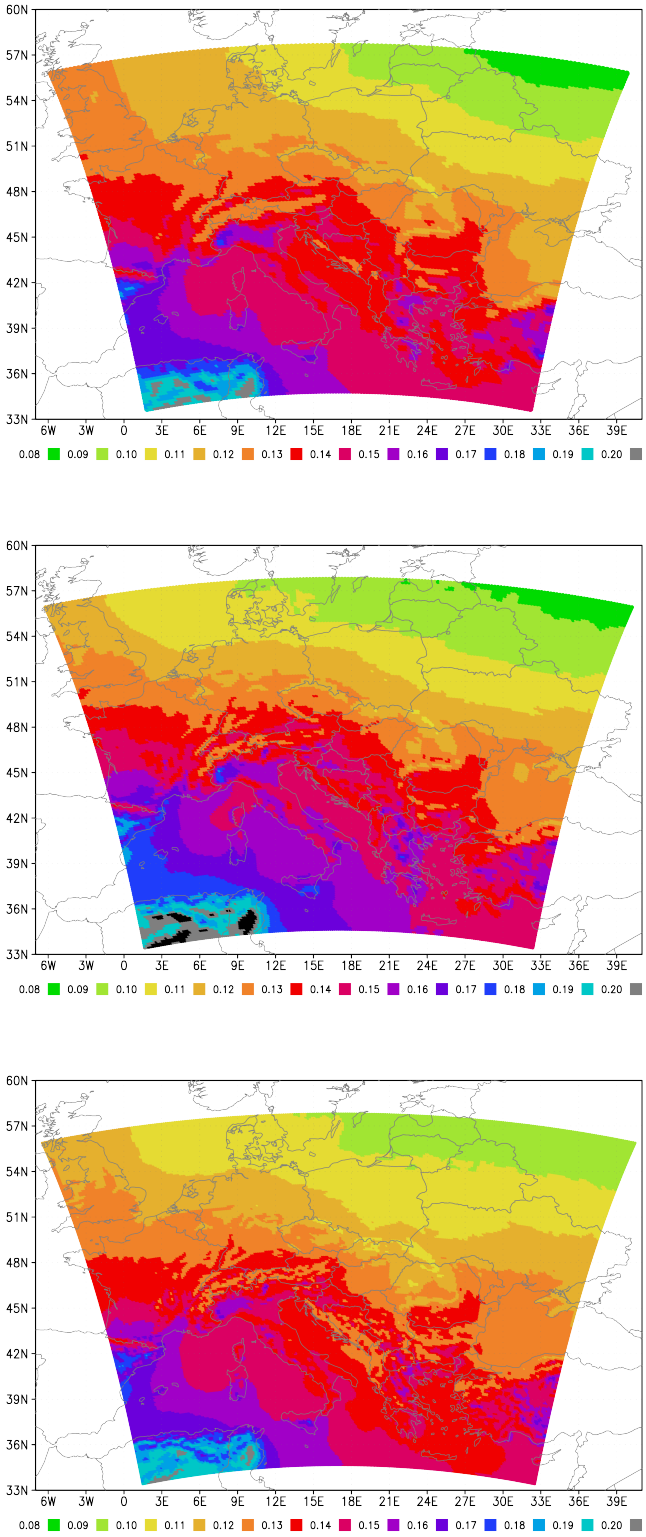

Figure 1.4: Average MCUF field (units 0.001 hPa) from ARPEGE for different resolutions of the LACE coupling files: (a) 20.678 km averaged for the period 23^{rd} Jan 2006 to $6th$ Feb 2008. (b) 15.4 km averaged for the period 6^{th} Feb 2008 to 11^{th} May 2010. (c) 10.51 km averaged for the period 11^{th} May 2010 to 15^{th} Nov 2014.

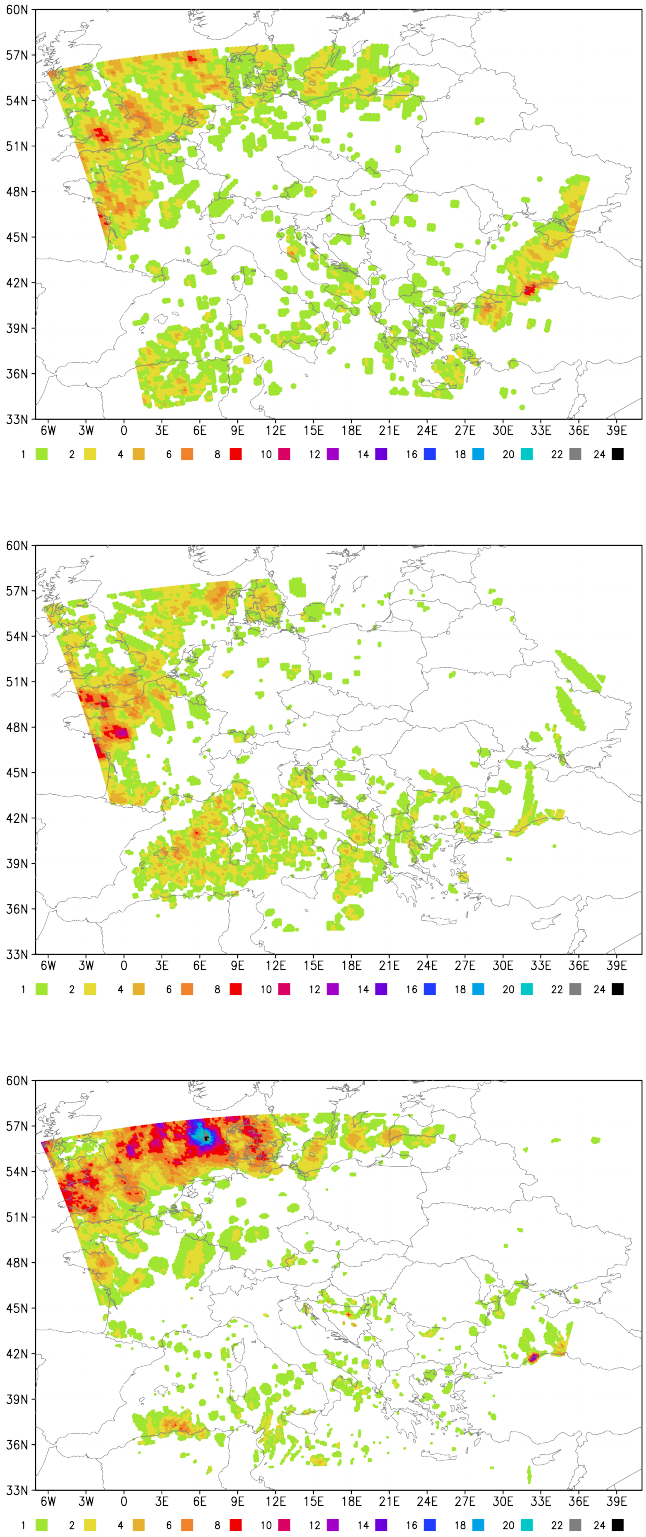

Figure 1.5: The number of times the MCUF field from ARPEGE exceeds 0.003 threshold for different resolutions of the coupling files: (a) 20.678 km averaged for the period 23^{rd} Jan 2006 to $6th$ Feb 2008. (b) 15.4 km averaged for the period 6^{th} Feb 2008 to 11^{th} May 2010. (c) 10.51 km averaged for the period 11^{th} May 2010 to 15^{th} Nov 2014.

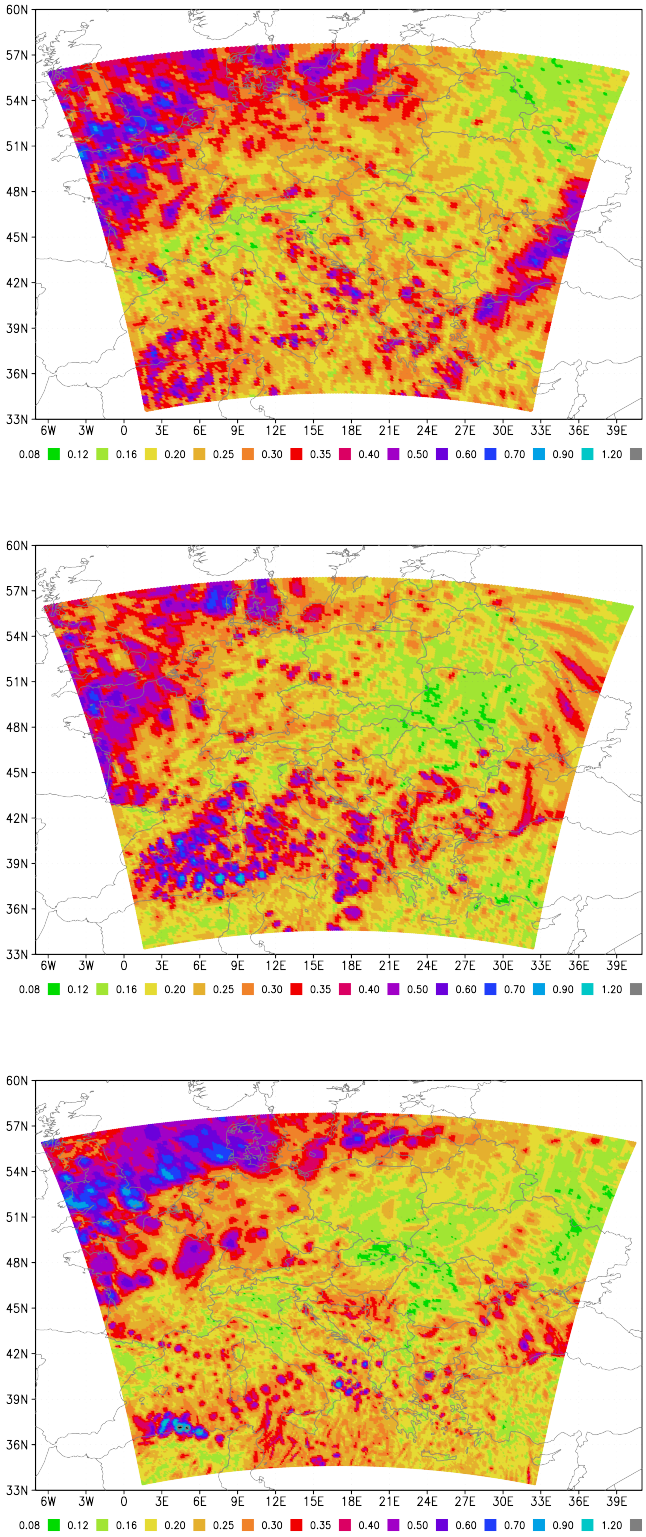

Figure 1.6: Absolute maximum values of the MCUF field (units 0.01 hPa) from ARPEGE for different resolutions of the coupling files: (a) 20.678 km averaged for the period 23^{rd} Jan 2006 to $6th$ Feb 2008. (b) 15.4 km averaged for the period 6^{th} Feb 2008 to 11^{th} May 2010. (c) 10.51 km averaged for the period 11^{th} May 2010 to 15^{th} Nov 2014.

1.5 Detecting rapidly moving pressure disturbances (RMPDs) in the ECMWF coupling files

MCUF is not computed by operational IFS, the alternative methods of detecting RMPDs have been tested on the coupling files received operationally from ECMWF.

1.5.1 Computing MCUF by running ALADIN model on the coupling files from IFS

MCUF computed by running ALADIN in the resolution of the coupling files from IFS using interpolated IFS analysis as the initial conditions (without any filtering) for 4 runs per day up to 78 hours forecast with 3 hourly output. The MCUF field computed this way is referred to as IFSM. The initial IFSM values are zero. IFSM computed during the first 3 hours of forecast has very large values due to model spin-up so only the fields corresponding to the 6 hour forecast and longer are used in the analysis.

The time series of IFSM maxima

The time series of the maximum values of IFSM field from the whole LACE domain for forecast ranges from 6 to 78 hours are shown in Figure 1.7 for the period from 27th October 2010 until 15th November 2014. The critical value is exceeded in 698 files (out of total 147350 files) during the 4 year period and over the whole domain (see Table 1.1). This is less often than in ARPEGE, since during the same period MCUF was larger than 0.003 in 995 files (out of 129674 files). The total number of files is larger for IFS than for ARPEGE since ARPEGE forecast LBC files extend up to 72 hours (and only 60 hours for the 18 UTC run), while files from all runs of IFS extend up to 78 hour forecast.

Although the critical value of 0.003 is exceeded less often with IFSM than with MCUF in ARPEGE, there are periods with large values associated to RMPDs during every part of the year, more often in autumn and the least often in summer. A figure with mean sea level pressure from the IFS coupling file and gridpoints with large IFSM values were plotted for each coupling file for which IFSM exceeded the critical value in order to estimate if the large IFSM values are associated to the cyclones in the IFS files (and not only in the ALADIN forecast run used to compute the IFSM field). Inspection of

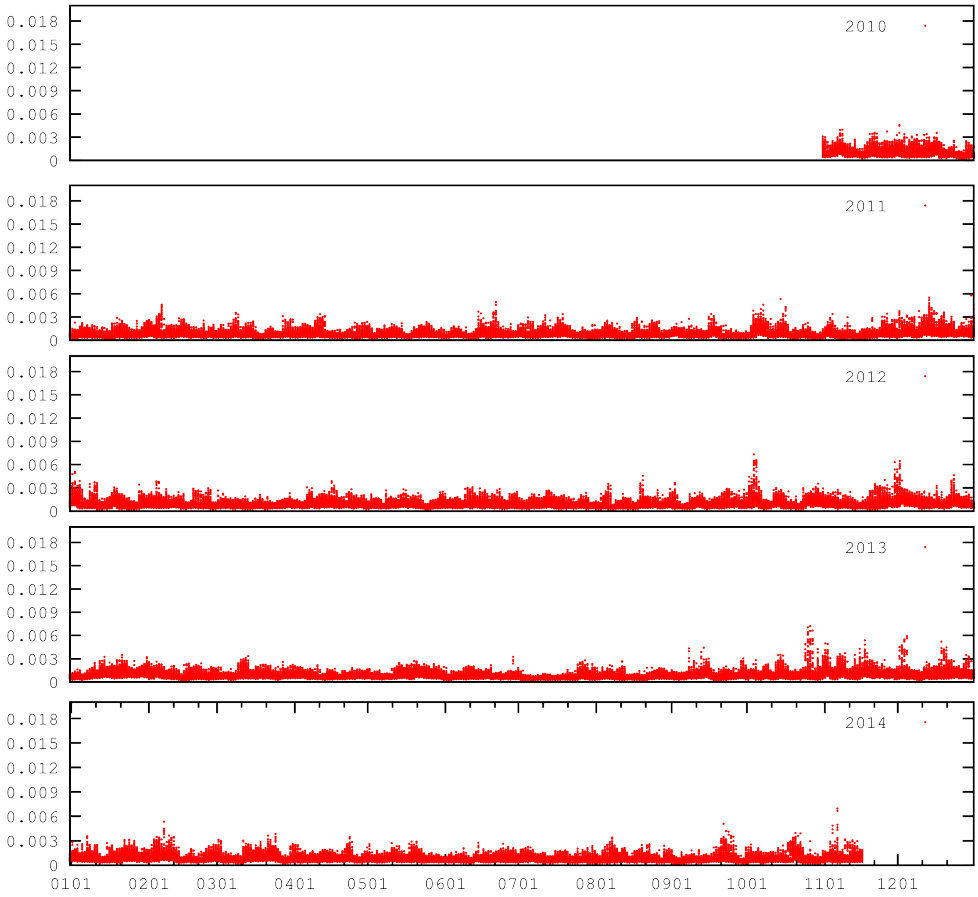

Figure 1.7: Time series of maximum value of IFSM field (units hPa) on the coupling LACE domain for 6 hour forecast up to 78 hours forecast, computed by running ALADIN, starting from 00, 06, 12 and 18 UTC analyses, since 1st November 2010 until 15th November 2014.

this set of figures lead to a conclusion that large values of IFSM are connected to a pressure low in IFS fields.

One should keep in mind that the MCUF values are computed by running ALADIN using IFS coupling files (initial and forecast). ALADIN model can yield different evolution of model variables, including surface pressure, so that large MCUF values correspond to a cyclone that moves quickly in the ALADIN forecast, not neccessarily in the IFS forecast. On the other hand, a RMPD in the IFS forecast might be less intensive or slower in the ALADIN forecast due to differences in the model set-up, choices in physics and dynamics.

Spatial distribution of IFSM

MCUF was computed by running ALADIN forecast on a limited area domain in 15.4 km resolution. Coupling zone was 8 points wide. The procedure could have missed a cyclone entering the LACE domain during the coupling interval. It is also expected to get unwanted phenomena in the IFSM field in the coupling zone of LBC files.

In the figure 1.8, a small dot is plotted in the position of each model grid-point in the colour corresponding to the average IFSM value multiplied by 1000 as shown in the colour scale below. Average IFSM field and average MCUF from ARPEGE for the same period (Figure 1.8) have substantially different spatial distributions. The differences are most pronounced over the Baltic area, where IFS yields more fast cyclones and over Mediterranean, where ARPEGE forecasts more RMPDs.

Maximum MCUF has larger values than IFSM (Figure 1.9). The average values are low along lateral boundaries, but the maxima do not decrease towards the lateral boundaries (Figure 1.8). The differences in the maximum MCUF and IFSM values are much less pronounced than for the averaged fields.

In most of the domain, MCUF and IFSM exceeded the critical value less than once in the 4 year period (Figure 1.10). The most critical part is in the north, where cyclones apparently traverse rather quickly and the number of files where IFSM s larger than threshold threshold exceeds 20. Both MCUF and IFSM show areas where pressure disturbances move more rapidly and/or frequently than elsewhere, such as the North Sea, the Baltic, western Mediterranean and west coast of the Black Sea. The critical value of 0.003 is exceeded more often for IFSM than in ARPEGE (Figure 1.10), over the North Sea, western Black Sea and the Baltic, but less often over the western Mediterranean. This suggests that IFSM field could be missing some of the RMPDs approaching Adriatic Sea and Croatia over the western Mediterranean.

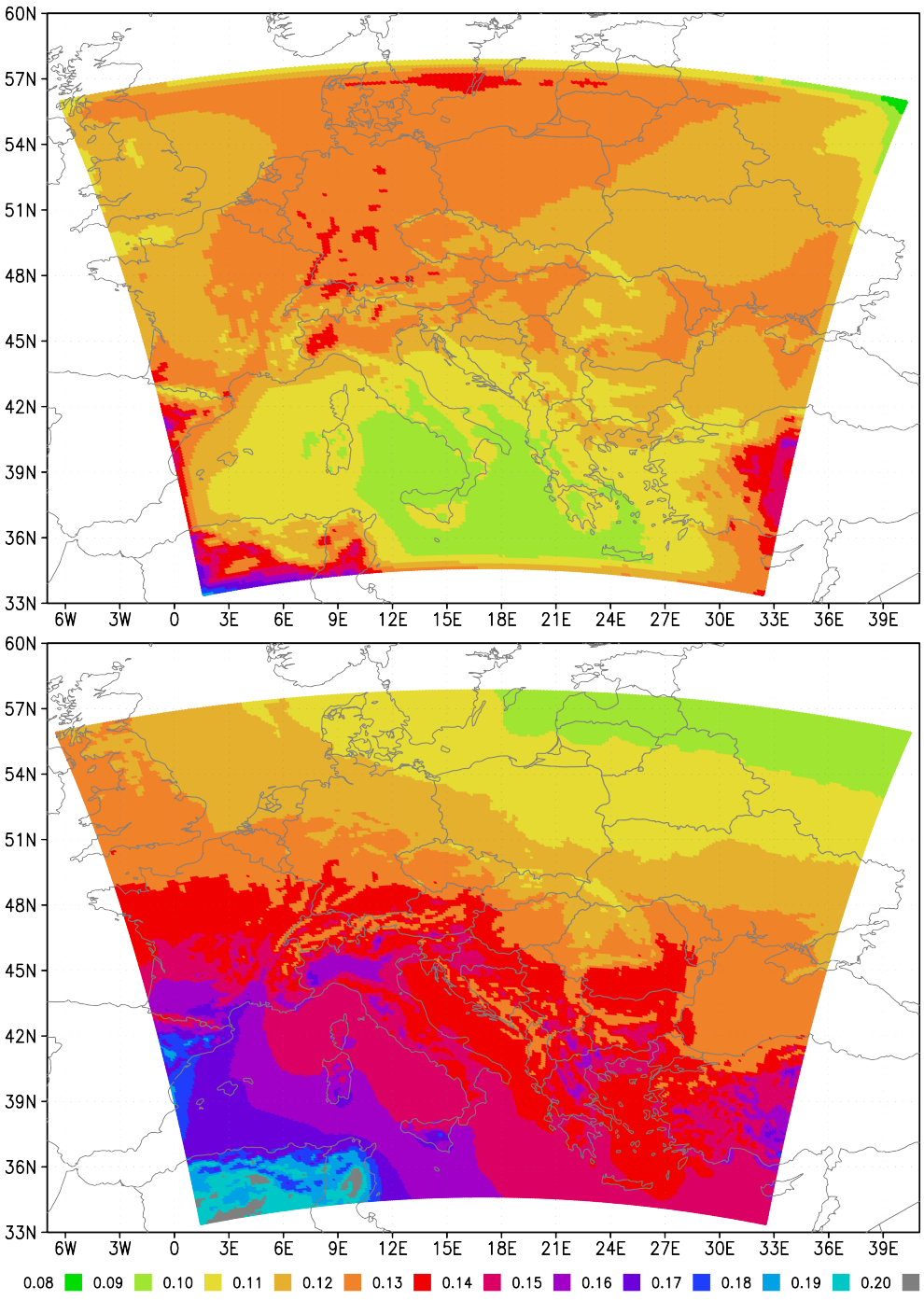

Figure 1.8: Spatial distribution of the average IFSM (top) and MCUF (bottom) values (units 0.001 hPa) for forecast hour greater than or equal to 06 hours for the period since 1^{st} Nov 2010 until 15^{th} Nov 2014.

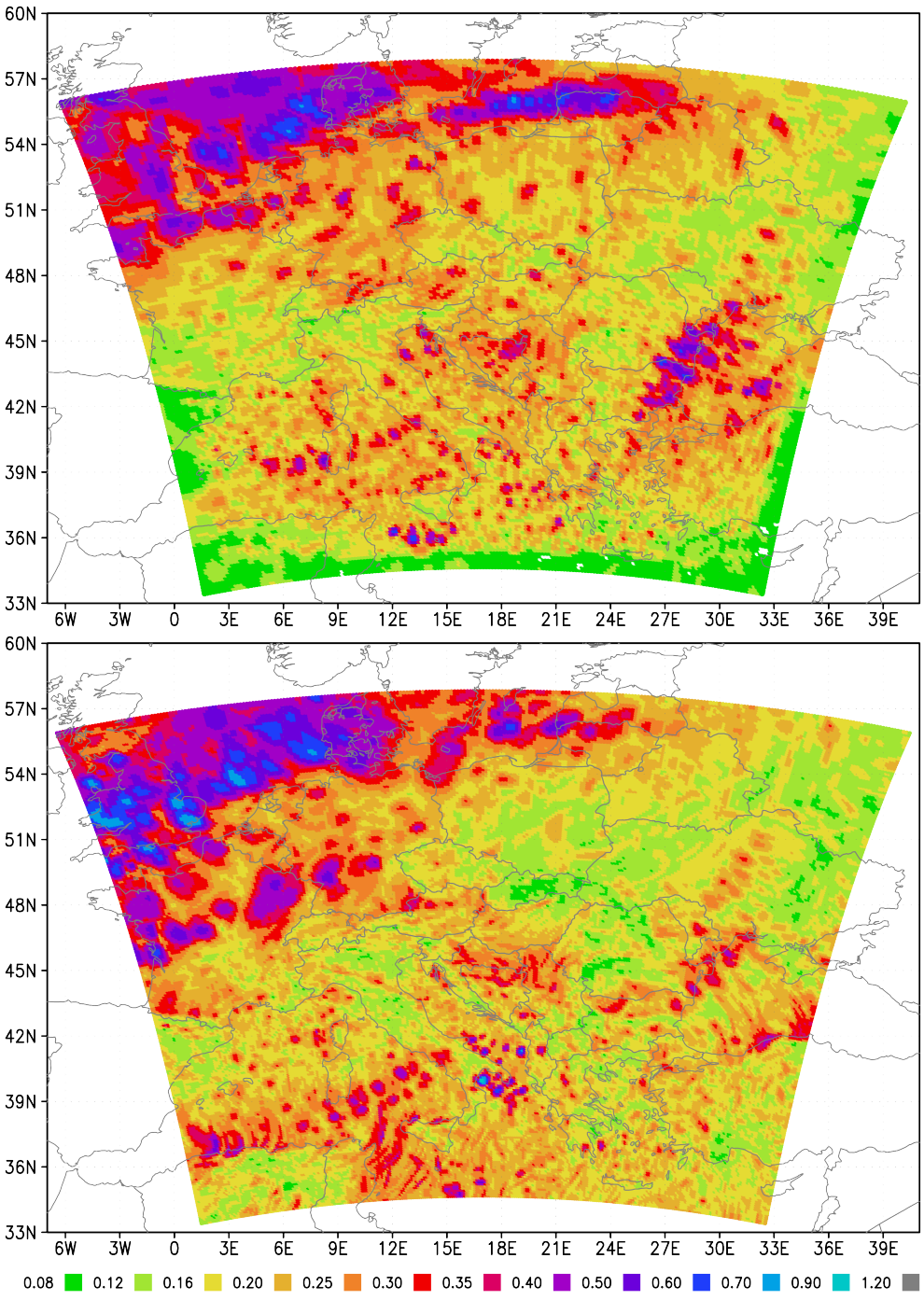

Figure 1.9: Spatial distribution of the maximum of absolute IFSM (top) and MCUF (bottom) (units 0.01 hPa), for forecast hour greater than or equal to 06 hours for the period since 1^{st} Nov 2010 until 15^{th} Nov 2014.

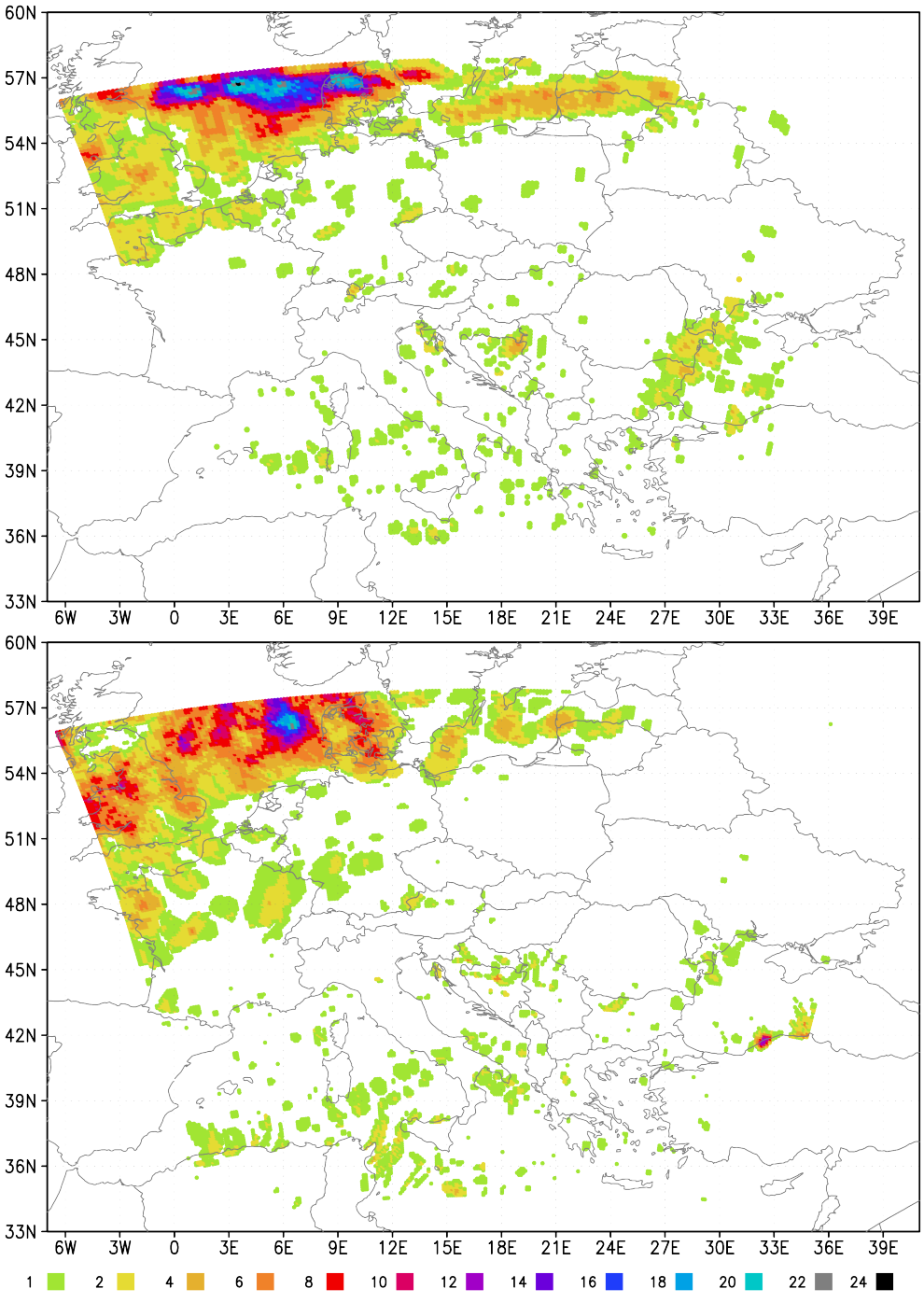

Figure 1.10: Spatial distribution of the number of occurences when IFSM (top) and MCUF (bottom) values exceed the value 0.003, for forecast hour greater than or equal to 06 hours for the period since 1^{st} Nov 2010 until 15^{th} Nov 2014.

Computing MCUF by running ALADIN model on the coupling files from ARPEGE

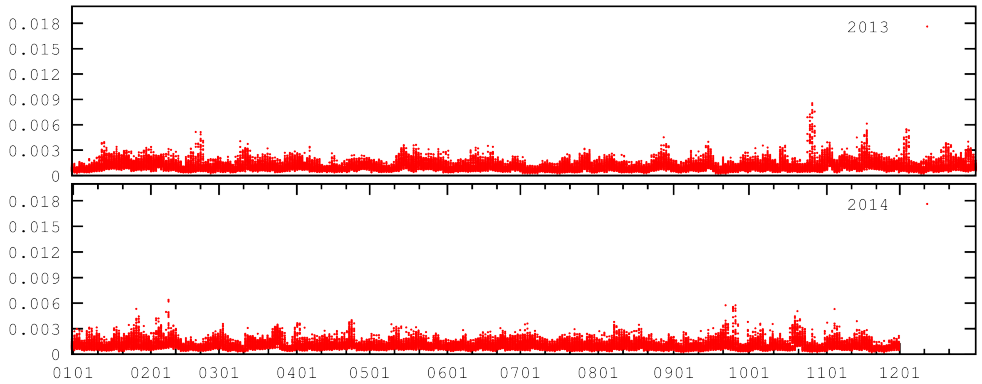

Figure 1.11: Time series of maximum value of ARPM (MCUF computed by running ALADIN on the coupling LACE domain from ARPEGE (the domain and resolution of LBC files) with 450 sec time-step).

ARPM was computed by running ALADIN on the domain and resolution (10.61km) of the ARPEGE coupling files with 450 seconds time step starting from the ARPEGE analysis without initialization. The time series of ARPM maxima over the LBC domain are shown in Figure 1.11. There is a good agreement with MCUF computed in ARPEGE. But ARPM gives additional strong signal for the storm that hit Turkey on 27th September 2014. MCUF did not show a signal for the same case.

1.5.2 The error function values using mean sea level pressure from ECMWF coupling files

ALADIN was run for one time step using fields from the coupling files from IFS as initial conditions in order to estimate the tendency of the model variables (in particular the surface pressure). The run is performed on the grid of the coupling files using 600 second time step. The error is estimated according to equation 1.1 and its maximum over the model domain according to the equation 1.2. The error function was computed for the period since 27th October 2010 until 15th November 2014 for experiments without initialization and initialized with SSDFI, and for the period since 1st January 2013 for the experiment with DFI.

Tendencies computed without filtering initialization

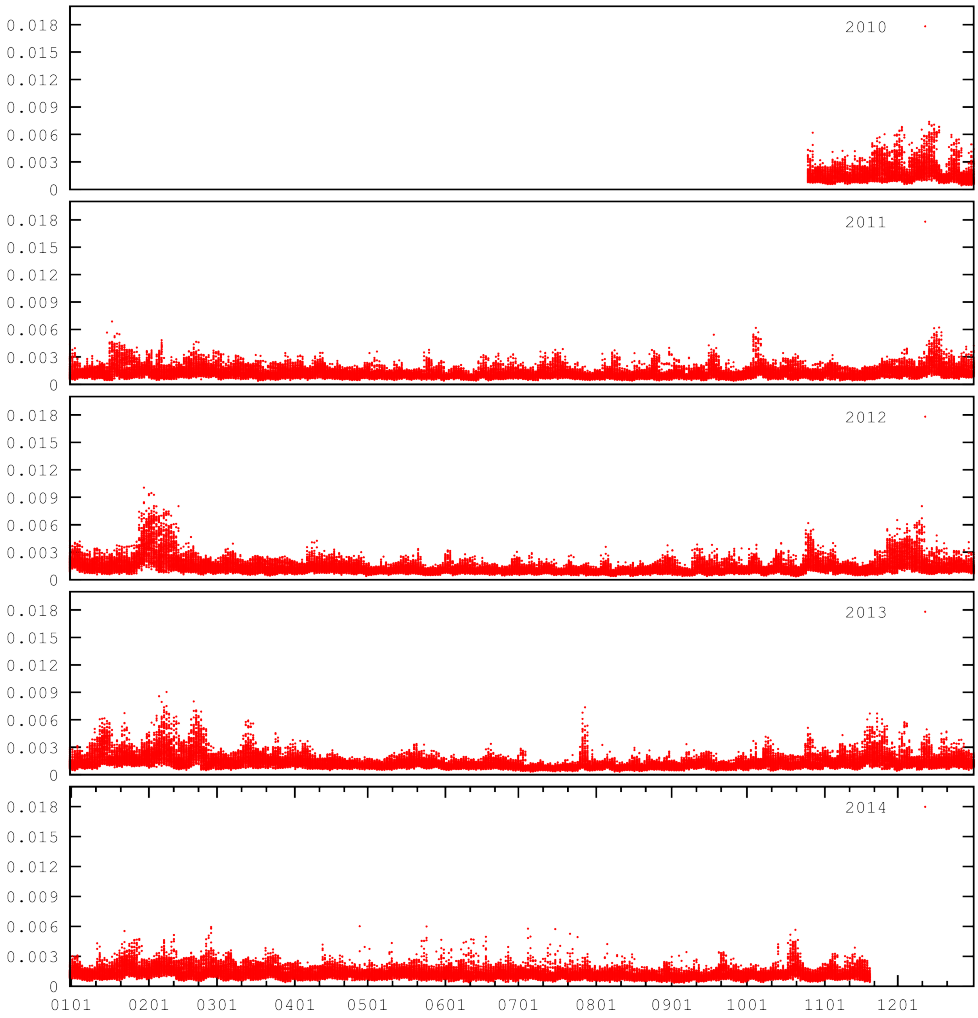

Figure 1.12: Time series of maximum value of error function (E_T, Eq. 1.2) without any filtering initialization.

The time series of E_T computed without initialization is plotted in Figure 1.12. The noise is more intensive than with IFSM, but the signal of RMPDs can be seen. The level of noise is lower in summer than in winter and it is lower when the error function is computed using mean sea level pressure than for surface pressure. Due to rather high level of noise, a critical value larger than 0.003 should be defined in order to avoid false alarms. The method using error estimate sometimes yields large values over mountainous

areas. If the model domain is defined so that the mountains are not in the intermediate zone (close to lateral boundaries), these events could be ignored by the operational procedure and would not be false alarms.

Tendencies computed with digital filter initialization

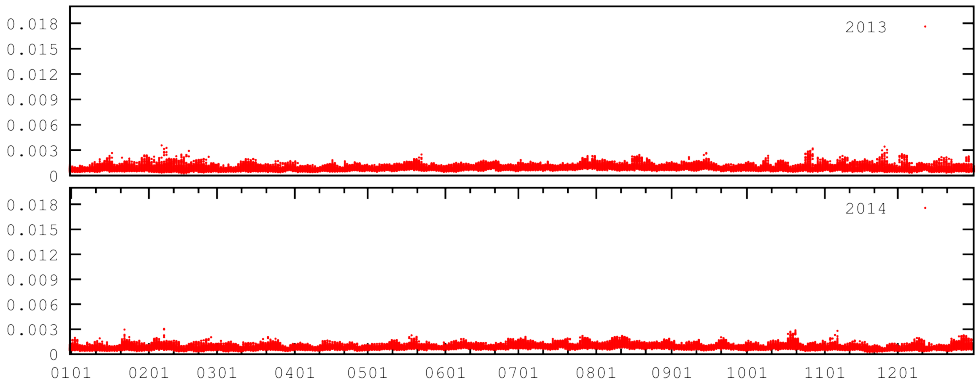

Figure 1.13: Time series of maximum value of error function, fields are initialized with DFI.

The time series of E_T computed for fields initialized with DFI is plotted in Figure 1.13 for the period from 1st January 2013 until December 2014. The noise is much lower than for the test without initialization, but the signal of RMPDs is also weaker. There is more noise in E_T computed for mean sea level pressure than for surface pressure in winter and spring, but less in the autumn. The signal of the RMPDs is removed almost completely from the error function computed for surface pressure, especially in winter and spring.

There is a signal for RMPD in E_T computed from mean sea level pressure on 27th November 2013 that does not exist in the time series of E_T for the surface pressure. The peak is located over the Alps and shows preristently for model runs from successive analyses about the same time (9 to 15 UTC that day). The satellite figures of the area for that date show clouds associated to mountain waves (not shown).

Tendencies computed with scale selective digital filter initialization

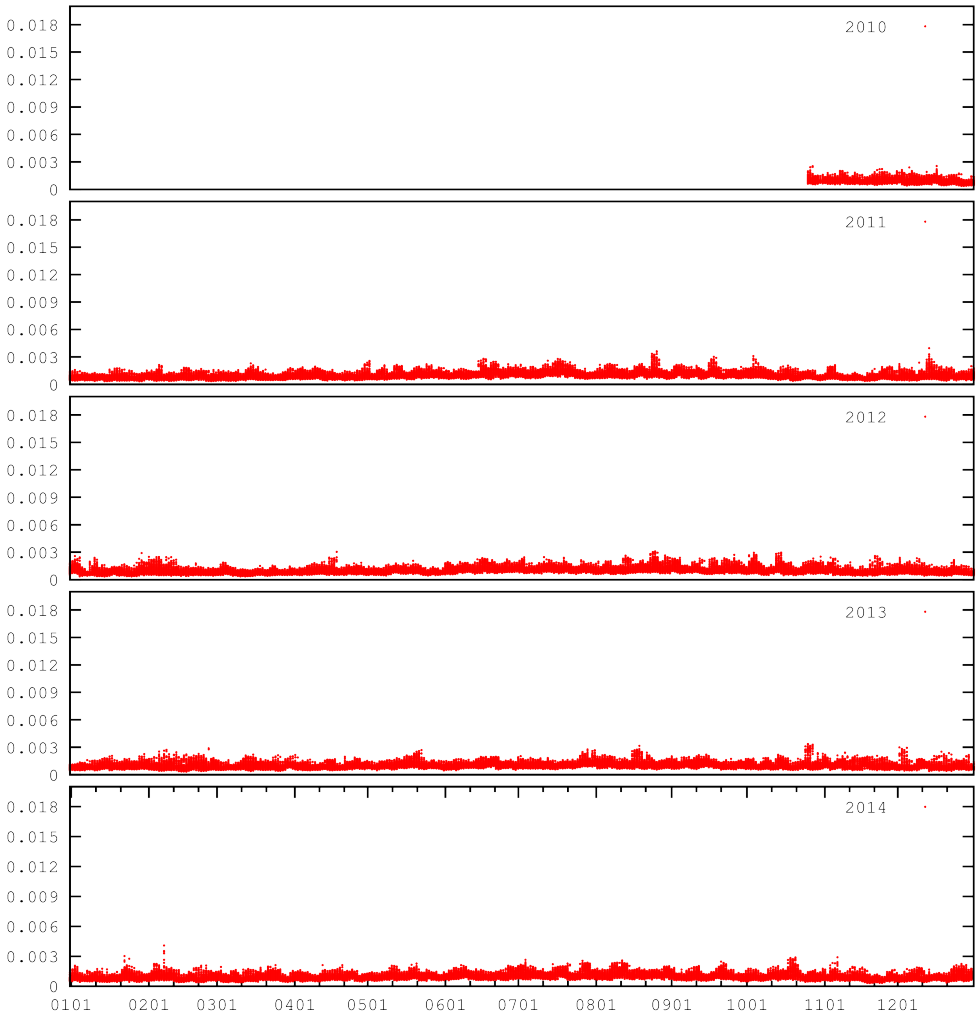

Figure 1.14: Time series of maximum value of error function, fields are initialized with SSDFI.

Similarly, the error function was computed after the fields in the coupling files have been initialized using SSDFI for the period since 27th October 2010 until December 2014. The time series of the maxima of the error function is ploted in Figure 1.14. The level of noise and the intensity of the signal of approaching RMPDs are similar to tose computed with DFI. But there are subtle differences. Several cases of RMPDs are more pronounced and there is no signal on 27th November 2013 that occured when DFI was used.

1.5.3 Amplitude of oscillations in mean sea level pressure

The amplitude of oscillations in mean sea level pressure was computed for the coupling files from IFS for the period since 27th October 2010 and for the coupling files from ARPEGE since 1st January 2013, both until December 2014. The time series of the maxima in the amplitude of the mean sea level pressure variations from IFS is displayed in Figure 1.15 and for ARPEGE in Figure 1.16.

Although the amplitude maxima achieve large values during periods without RMPDs (the periods without RMPDs are those when MCUF and IFSM are low), the amplitude is so much larger in a case with RMPD that there is a signal that can be distinguished in the noisy pattern.

A figure was plotted with mean sea level pressure from the coupling file from IFS and all points with large values of A ($A > 0.003$) for each case when this threshold was exceeded. The majority of the cases are related to propagating cyclones and pressure throughs and are usually associated to the large values of IFSM. However, there are cases when A is larger than the threshold in mountainous regions of Alps, Atlas mountains and Turkey, but these are associated to an atmospheric front approaching the area so the large values could not be dismissed as false.

There is also a number of cases when IFSM did not indicate a RMPD, while A did reach values above the threshold in points close to the edge of the coupling domain. The subsequent coupling times also had large values of A in the vicinity. In these cases, the cyclone entered the coupling domain too quickly to be detected by the procedure used to compute the IFSM field.

1.6 Conclusions

The three hourly coupling update interval is insufficient for resolving the storm in lateral boundaries as presented for the Lothar storm case ([Termonia(2003)]). [Davies(2014)] recommends choosing carefully the resolution and fequency of large scale LBCs. However, meteorological services that depend on LBCs from elsewhere might have little choice. A coupling update frequency is sufficient if the large scale model data contains only features that are large enough and slow enough to be resolved by the coupling update period ([Denis et al.(2003)]). Therefore, the coupling update frequency is determined by the properties of the global model, not the LAM that uses it for LBCs.

[Termonia(2004)] developed a strategy to monitor rapid changes in surface pressure in ARPEGE by producing a diagnostic output field for the filtered

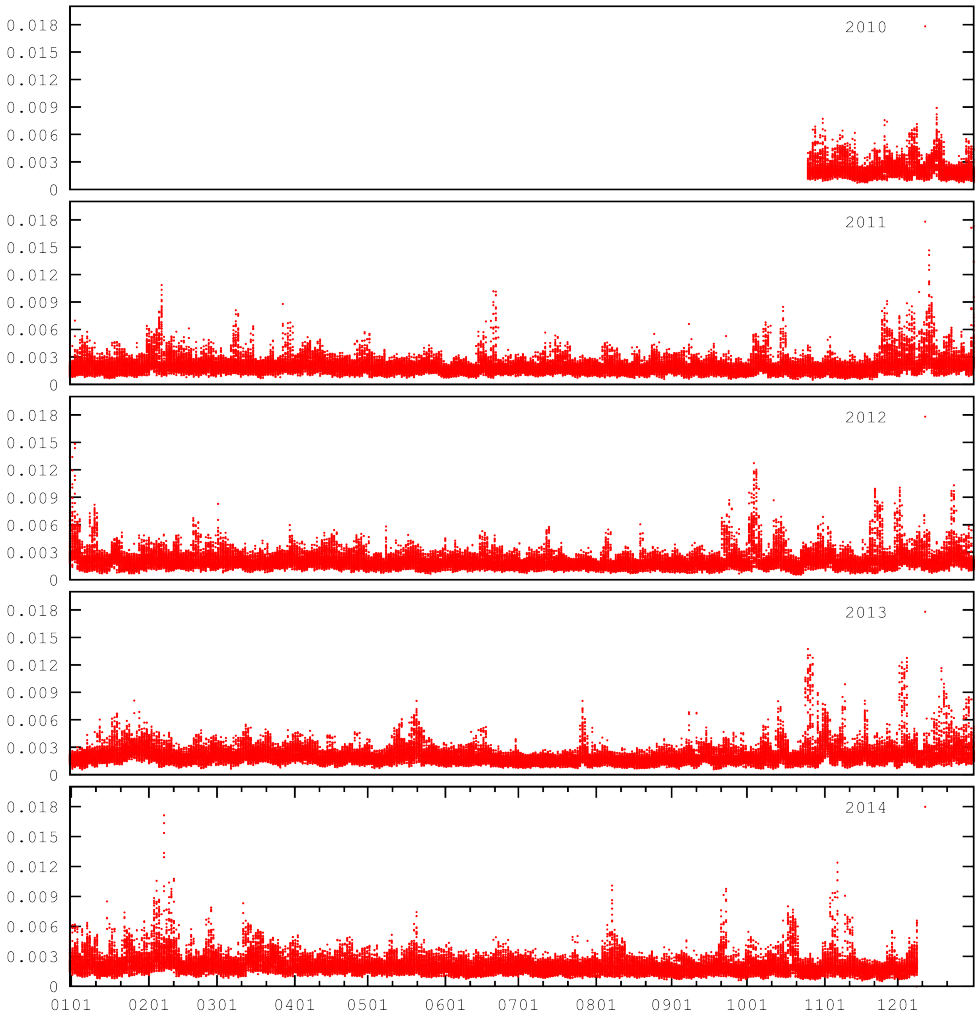

Figure 1.15: Time series of the maximum value of the amplitude in the mean sea level pressure variations (Eq. 1.3) computed from the coupling files from IFS.

surface pressure (MCUF). This field is provided in the coupling files since 06 UTC run on 23rd January 2006 for the LACE coupling domain.

When MCUF is larger than a threshold value of 0.003 ([Termonia(2004)]), there is a rapid development in the surface pressure suggesting that a fast cyclone has moved through the area. If the point with the large value is inside the coupling zone of the ALADIN domain, it can be expected that the ALADIN model run will miss the cyclone strength and development due to time interpolation of boundary data. When the time series of MCUF data

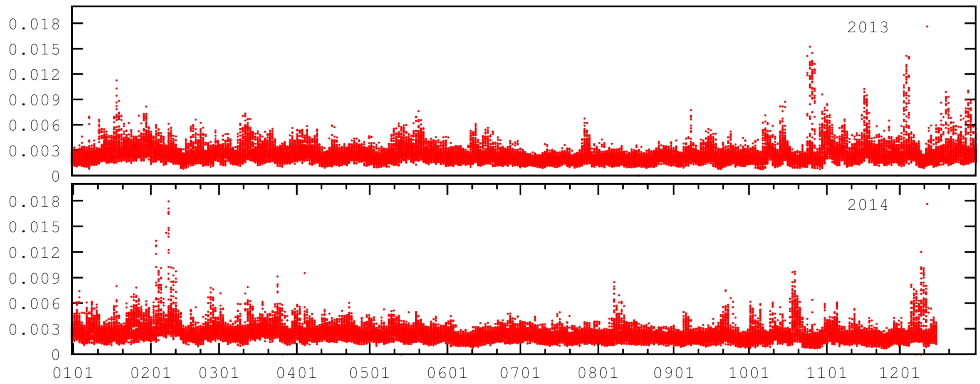

Figure 1.16: Time series of the maximum value of the amplitude in the mean sea level pressure variations (Eq. 1.3) computed from the coupling files from ARPEGE.

has been analysed for the Belgian domain ([Termonia et al.(2009)]), it was found that such events occurred only several times per year.

The analysis of the MCUF field in this article shows that this field is above the threshold more frequently for the whole LACE coupling domain as well as for the coupling zone of the Croatian operational domain (it covers larger area than the operational Belgian domain in ([Termonia(2003)]), but the event can still be considered rare. There are changes from one season to another (more ot less 'stormy'), but there is no apparent increase in the number of fast propagating storms with an increase of the ARPEGE resolution (at least in the range of resolutions available for this study).

The spatial distribution of MCUF reveals that RMPDs favour the sea surfaces, especially the North Sea and the western Mediterranean. Analysis of the MCUF and IFSM fields for a longer period can show which areas favour quickly moving storms that could be missed by the coupling procedure if the 3 hourly coupling period is used. Maps with number of occurrences when the filtered pressure field is larger than the 0.003 threshold show that there are not to many places where to put the coupling zone in order to avoid LAM forecast failure in the case of a RMPD. The problem would be only made worse in higher resolution LAM. The coupling zone on the lateral boundaries is 8 grid points wide and shrinks with the resolution increase. The storm needs less time to cross the narrow coupling zone. Higher resolution global model can yield more intensive pressure changes.

The spatial distribution can be viewed as a map of the fast cyclone tracks and areas that support rapid changes in cyclone development. Not surprisingly, this study shows that not only North Sea, but also the western Mediter-

ranean is an area where storms frequently propagate with high velocities and can not be resolved in LBCs of a 8 km resolution LAM when provided with 3 hour interval. In LAM with roughly 3 times larger horizontal resolution, even 1 hour coupling interval would be insufficient.

There is no field similar to MCUF provided in the coupling files of IFS from ECMWF. Therefore an experiment has been performed in order to compute the field locally from the coupling files. The forecast needed to compute MCUF was run using ALADIN model and the resulting field IFSM can be used for detecting RMPDs in the operational forecast. It requires running the ALADIN forecast in low resolution up to 78 hours (same range as the coupling files are provided). It is more computationally expensive than reading the field already provided in the LBC files but it is feasible. However, the results contain some detrimental effects:

- different model dynamics could lead to different developments in the surface pressure field and hence different MCUF values,
- a quickly moving storm can enter the LBC domain undetected and consequently be missed by the MCUF,
- rather low cyclone activity on the western Mediterranean comapred with results using ARPEGE.

The error function ([Termonia(2003)]) were computed using tendencies estimated by running ALADIN for one time step, using fields from the coupling fields without initialization, initialized with DFI and with SSDFI. No initialization yields a signal of RMPDs but also a lot of noise. Clearly a higher threshold value should be used, but it should be chosen carefully. DFI reduces the level of noise and the magnitude of the signal and many RMPDs are removed from the time series (Figure 1.13) but there are still evidences of large values related to mountains. SSDFI reduces the level of noise and the signal of RMPDs, but more of the signal is preserved.

Finally, RMPDs are detected by simple computations of variations in the mean sea level pressure from three consecutive coupling files. Apparently, this rather simple method can be used for detecting RMPDs. The noise is more intensive than for error function computed without initialization, but so is the signal for RMPDs. This method can be used on any variable and it does not require running any model using coupling data as initial conditions. Mean sea level pressure is less sensitive to the reduction in the coupling update frequency than precipitation and vorticity ([Denis et al.(2003)]).

Climate LAMs could benefit from a large domain ([Žagar et al.(2013)]). It takes several days for the cascade of variance to fill the small scales

([Laprise(2008)]). Loosing small scale features, arriving from the global model at lateral boundaries, certainly does not help. If the domain of the climate LAM is small and the flow over the area is strong, it could move over the domain too quickly to develop small scales ([Žagar et al.(2013)]), and if the temporal interpolation of LBC data filters high resolution data from a global model, there might not be enough space (in the domain) nor time (before the flow leaves it) for LAM to recreate these small scales.

On the other hand, NWP models that have small scale data in the initial conditions through blending ([Brožkova et al.(2001)]) or data assimilation cycle (eg. [Stanešić(2011)]) need RMPDs that enter the domain during the model forecast. It took ALADIN 66 hours to develop a small scale feature in the 2km resolution nonhydrostatic run ([Tudor and Ivatek-Šahdan(2010)]) coupled to 8km operational forecast that was run without data assimilation at the time ([Ivatek-Šahdan and Tudor(2004)]).

As there are plans to increase the resolution of the operational ALADIN to 4km and ECMWF announced plans for the increase in the horizontal resolution of operational IFS, the problem of resolving RMPDs in LBC data available with 3 hourly interval will become more frequent and it is questionable if hourly coupling data would be sufficient in some cases. Boundary error restarts ([Termonia et al.(2009)]), gridpoint nudging ([Termonia et al.(2011)]), computing corrected interpolation in time with time derivatives ([Termonia(2003)]) and alternative methods of interpolating LBC data in time ([Tudor and Termonia(2010)]) are computationally expensive and should be used only when needed. Therefore such cases should be detected by a reliable method since any missed case means that LAM would not forecast severe weather conditions. The error function computed without initialization and the amplitude method (Section 4.3) are cheap methods that could be applied in a straightforward manner. MCUF from IFSM seems reliable for most of the LACE domain. The error function computed from the initialized fields does not improve the results enough to justify the extra computational cost. The alternative is to compute MCUF in operational IFS.

Chapter 2

Including LBCs into LAMs

Alternative formulations for incorporating lateral boundary data into limited area models

2.1 Abstract

Limited-area models (LAM) use higher resolutions and more advanced parameterizations of physical processes than global numerical weather prediction models, but suffer from one additional source of error - the lateral boundary conditions (LBC). The large scale model passes the information on its fields to LAM only over the narrow coupling zone at discrete times separated by a coupling interval of several hours. The LBC temporal resolution can be lower than the time necessary for a particular meteorological feature to cross the boundary. A LAM user who depends on LBC data acquired from an independent prior analysis or parent model run can find that usual schemes for temporal interpolation of large scale data provide LBC data of inadequate quality. The problem of a quickly moving depression that is not recognized by the operationally used gridpoint coupling scheme is examined using a simple one-dimensional model. A spectral method for nesting a LAM in a larger scale model is implemented and tested. Results for a traditional flow-relaxation scheme combined with temporal interpolation in spectral space are also presented.

2.2 Introduction

Limited area models (LAMs) are used as an alternative to global numerical weather prediction (NWP) models for a wide variety of research and operational forecast applications. Particularly LAMs are subject to different

sources of forecast error: the parameterizations of physical processes, the initial conditions, the numerical algorithms and surface forcing. These also affect various global NWP models, but LAMs have one additional source of error related to their lateral boundary conditions (LBCs). The most popular scheme for LBC treatment is the the one proposed by [**?**], used almost exclusively for one-way coupled operational LAMs [**?**]. There are problems that are linked with the nature of various lateral boundary schemes [**?**] but LBC problems can also be of a different source, for example the quality of the large scale data. An overview of the weaknesses of the LAM forecast caused by the LBCs was provided by [**?**].

LBCs are obtained from models with a coarser mesh in the horizontal and the vertical that usually use simpler (different) parameterizations of physical processes. The coarse grid of the host model smooths the information supplied at the lateral boundaries [**?**]. The numerical procedures used on the interface of the two grids also generate errors [**?**]. [**?**] showed that commonly used temporally interpolating lateral-boundary data may lead to errors in the surface field of up to about 10 hPa in case of fast propagating storms.

Model errors due to LBCs can be significant since it propagates into the domain interior during the forecast [**?**]. It propagates and amplifies as it enters the domain of integration depending on the intensity of the cross-boundary flow and spreads further through the domain with longer time of integration [**?**]. This problem is becoming more important as LAM forecasts tend to be longer, up to 72 hours and in higher resolution, covering smaller area and with narrow coupling zone. Enlargement of the domain to move the edges far from the area of interest does not prevent the LBC error from eventually contaminating the solution [**?**].

[**?**] developed a regional spectral model that predicts deviations from the global model forecast and find that shorter coupling intervals allow more noise in the mean sea level pressure field along lateral boundaries, but not in the precipitation field. In order to force the perturbations to zero along lateral boundaries and reduce the aforementioned noise, they apply lateral boundary relaxation for the dynamical part of the total tendency and a blending of the total tendency over the entire regional model domain. The second procedure was found unnecessary for noise removal. The subsequent study [**?**], using the same model, revealed that it is not necessary to have large domain in order to avoid lateral boundary influence and multi nesting is not necessary for a very fine resolution forecast over a small domain. Assignment of lateral boundary values at the boundaries is found essential for representing scales too large to be periodic on LAM domains [**?**], which represents a large scale closure.

The schemes for lateral boundary conditions used in NWP usually spec-

ify every field at all the lateral boundaries making the initial-boundary problem mathematically ill-posed [**?**]. Unfortunately, [**?**] found that local pointwise boundary conditions cannot be well-posed for hydrostatic equations and open boundaries. There are solutions in simplified models [**?**, see e.g.]]McDonald2000,TermoniaVoitus2008 that allow well-posedness and to control the gravity waves, but the extension of the gravity wave control mechanism from one to more dimensions leads to fundamental difficulties [**?**]. The search for the well-posed solution continued, e.g. for the problem in semi-Lagrangian models when the origin point of the trajectory lies outside of the model domain [**?**], the application of this work in spectral models [**?**, **?**], and improved schemes for overspecified LBCs such as for instance [**?**]. Spurious gravity waves that occur due to the ill-posedness of the LBCs are filtered by the coupling procedure itself and/or the horizontal diffusion scheme and it is supposed that the remaining spurious waves are acceptable. Even when the problem is well-posed, waves can still be reflected from the boundary. Boundaries that transmit waves in and out without spurious reflections are said to be transparent [**?**]. Such set has been tested in a nested environment on a simple set of shallow water equations [**?**] on a single level without diffusive terms. However, the results still depend on the quality of the large scale data used for coupling.

The quality of the LBC data for operational as well as research purposes is severely restricted since its amount is limited by storage and data-transfer capacities. Large scale fields are usually available in temporal resolution of several hours, but they are needed at each LAM time step which is usually on the order of several minutes. Consequently, LBCs are obtained at every LAM time-step using large scale fields that are interpolated in time. This interpolation procedure corrupts the fields, especially the features that have time scales shorter than the coupling interval. The situation can be made even worse when the large scale fields are taken only from the narrow area close to the domain lateral boundaries. Consequently, small scale features that are quick enough to enter the domain during one coupling interval are not suitably represented by the interpolated data, see [**?**].

In [**?**] it is shown that it is possible to detect boundary errors coming from such deficiencies in the interpolation. [**?**] proposed a solution that relies on a restart of the forecast after the storm has entered the domain and the error is detected by the boundary error procedure. This proposal improves the forecast itself, but still exhibits two weaknesses that may be subject for improvements. The first is that a standard initialization like the popular digital-filtering initialization (DFI) may weaken the depths of the large-scale storms present in the data of the coupling model. This can be controlled by using a scale-selective digital filter (SSDFI) as proposed in [**?**]. Secondly, any

small scale information that has been built up in the limited-area model since the beginning of the forecast run is lost. In that paper it is also suggested that this method may be improved in spectral models by relying on spectral nudging of the type proposed in [**?**], [**?**], [**?**], and [**?**]. In those papers the spectrally nudged information was used over the entire domain. Possible benefits of spectral nudginig have been noticed by [**?**]. The present paper makes a first feasibility study of such methods to improve the LBC temporal resolution problem, in particular investigating its use within the buffer zone at the lateral boundary of the domain only. As a comparison the spectral nudging over the entire domain will also be included in the present paper.

The aim here is to develop a simple coupling procedure that could be used operationally as a supplement or as an alternative to the flow-relaxation one either always, or when the quality of the LBCs is found insufficient by the monitoring procedure of [**?**]. Alternative time-interpolation schemes for LBC data are proposed. Alternative time-interpolation schemes for LBC data are proposed. Different coupling procedures are implemented and tested using a simple one-dimensional model. This enables the identification of the errors linked to a particular LBC schemes, that could hardly be identified using a realistic model [**?**].

This paper is organized as follows. Section 2 outlines the problem by discussing the time evolution of spectral coefficients produced by an operational run of a realistic three dimensional LAM. The one-dimensional model used for the testing of the alternative formulations, is also briefly the described in this section. Results obtained using the flow-relaxation scheme are presented in Section 3. The method of spectral coupling is described in Section 4. Section 5 describes the time interpolation done in spectral space in combination with the usual gridpoint coupling scheme. The final part of this paper brings discussion and conclusions.

2.3 Data and experimental setup

This section analyses spectral data of a forecast for the operational ALADIN limited-area numerical weather prediction model developed and maintained by the [?]. The obtained results will then be used as a basis for proposing improved temporal interpolation schemes in sections 4 and 5.

Figures 2.1a and 2.1b show the evolution of the mean-sea level pressure (mslp) of the Lothar storm [?] in an operational forecast of the ALADIN model between 0900 UTC and 1200 UTC 26 December 1999. This model was run with a resolution of $\Delta x = \Delta y = 9.5km$ and 300 grid points in the zonal and meridional directions and a time step of $\Delta t = 300s$. Fig. 2.1c shows the mslp in the middle of this time interval at 1030 UTC. When linearly interpolating this storm within the 3-h time interval between $t_0 = 0900$ UTC and $t_1 = 1200$ UTC,

$$\mathcal{L}\, c\,(t) = \frac{t_1 - t}{t_1 - t_1}\, c\,(t_0) + \frac{t - t_0}{t_1 - t_0}\, c\,(t_1)\ . \tag{2.1}$$

one gets at $t = 1030$ UTC not one, but a "dipole" of two depressions, as can be seen from Fig. 2.1d. In most operational applications such interpolated data is used as coupling data for the Davies scheme. If, for instance, the configuration in Fig. 2.1d would happen in the fictitious Davies zone shown in the panels c and d, some completely spurious information might enter the physical domain of interest.

ALADIN is a spectral model following the work of Haugen and Machenhauer (1993), so the Fourier components of the fields can be easily obtained. The spectral coefficients are computed on an extension of the physical domain of the limited-area model, where the fields on the extension zone are constructed in such a way as to make the fields periodic using splines. During a time step computation the spectral information is present at the beginning of the time step and during the inversion of the Helmholtz equation, as explained in table II of [?]. It is our aim here to investigate whether the spectral information may be useful to improve *the proposals made in [?].*

Within the ALADIN model a fast Fourier transform is applied twice in the two spatial horizontal directions I and J of the grid-point field F_{IJ} with gridpoint indices $I = 0, \ldots, M-1$ and $J = 0, \ldots, N-1$ by

$$c_{KL} \;=\; FFT\,[F_{IJ}]_{KL}\,\frac{1}{MN}\sum_{I=0}^{M-1}\sum_{J=0}^{N-1} F_{IJ}\, e^{-\frac{2\pi i}{M} I\, K} e^{-\frac{2\pi i}{N} J\, L}\,, \tag{2.2}$$

for the indices $K = -M2, \ldots, M2$ and $L = -N2, \ldots, N2$, corresponding to waves with wave lengths $l_{KL} = [(K/M\Delta x)^2 + (L/N\Delta y)^2]^{-12}$.

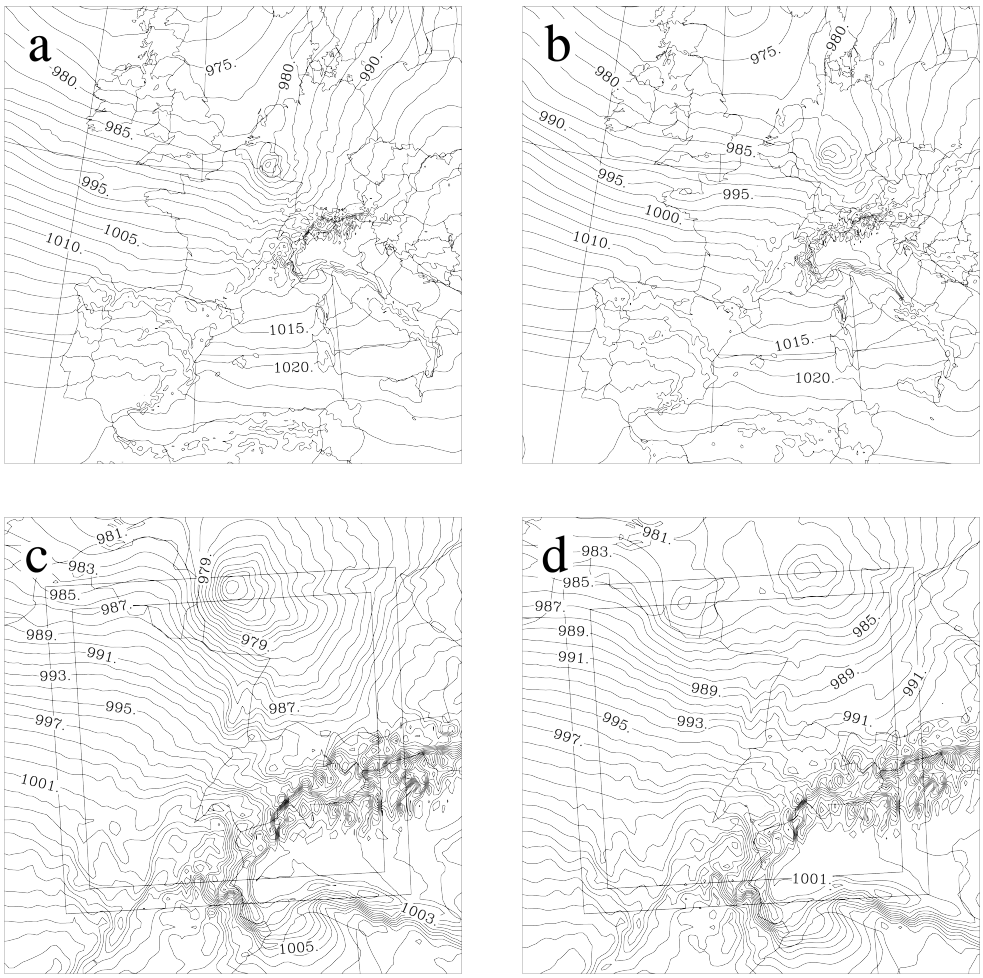

Figure 2.1: ALADIN-France forecast of the Christmas storm on 26 December 1999: (a) the MSL pressure at 09 UTC (contour interval is 2.5 hPa), (b) MSL pressure at 12 UTC (contour interval is 2.5 hPa), (c) the MSL pressure at 10h30 UTC, (zoom of the domain with contour interval of 1. hPa), and (d) the linear interpolation at 10h30 UTC between the MSL pressure at 09 UTC and the MSL pressure at 12 UTC (zoom of the domain with contour interval of 1. hPa). The frame on the Figs. c and d is a fictitious Davies relaxation zone containing the "dipole" structure of the interpolated field in Fig. d.

The spectral coefficients are available for each model time step in the interval $[t_0, t_1]$,

$$c_{KL}^{\alpha} = c_{KL}\left(\alpha \Delta t\right) \ , \tag{2.3}$$

for $\alpha = 0, \ldots, n_t$ corresponding to $t = t_0 + \alpha\Delta t$, with Δt the model integration time step. It can be easily verified that applying $\mathcal{L}$ to the grid-point field F_{IJ} is equivalent to applying it to the spectral coefficients c_{KL},

$$FFT\left[\mathcal{L}F_{IJ}\right]_{KL} = \mathcal{L}c_{KL}\,, \tag{2.4}$$

so the effect of the linear interpolation in Eq. (2.1) can be studied by investigating its effect on each separate spectral coefficient.

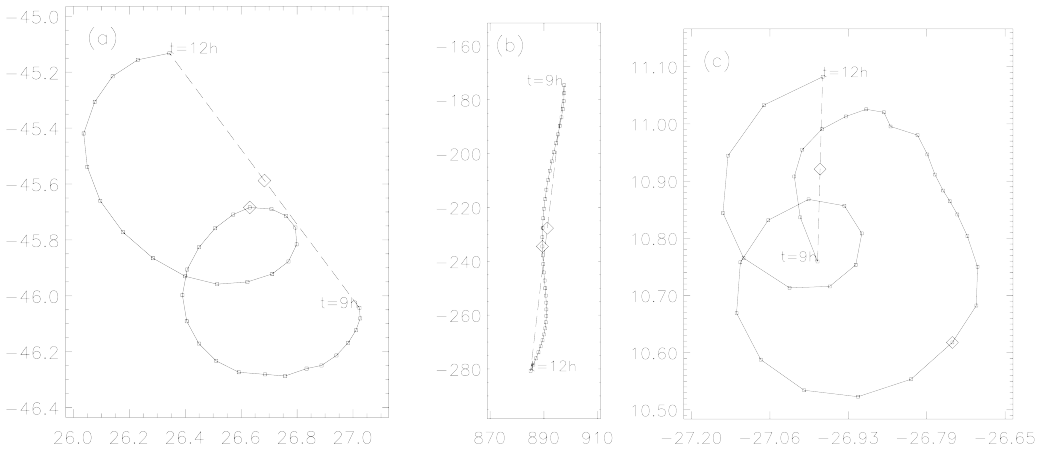

Figure 2.2: Example of the time evolution of three spectral coefficients: (a) $c_{11,-15}$, (b) $c_{1,0}$, and (c) $c_{18,3}$. The x axis and the y axis indicate the real and the imaginary part respectively, in units of Pa.

Fig. 2.2 shows the time evolution of the three coefficients $c_{11,-15}$, $c_{1,0}$, and $c_{18,3}$, for the surface pressure between time $t_0 = 9h$ and $t_1 = 12h$ forecast range of the forecast run presented in Fig. 2.1. It can be seen from the time evolution of $c_{11,-15}$ in Fig. 2.2a that even though the linear interpolation may be quite good in the middle of the interval (indicated by the diamonds), it can completely miss the rotating part of the time evolution of the spectral coefficient. So the interpolation should be considered in all points in the interpolation interval. Fig. 2.2b shows for the large scales, illustrated here by $c_{1,0}$ with a wave length of 2850 km, that the linear interpolation is a good approximation. On the other hand for the small scales, exemplified here by $c_{18,3}$ with wave length $l_{18,3} = 156\,km$, the interpolation is entirely wrong.

The time evolution of the spectral coefficients c^{α}_{KL} in Fig. 2.2 can be seen as a superposition of a linear trend and a rotation in the complex plane

$$F_{KL}(t) = \Phi_{KL}(t) + \mathcal{A}_{KL}(t)\,, \tag{2.5}$$

with the linear trend given by

$$\Phi_{KL}(t) \;=\; \phi_{KL}(t_0) + (t - t_0)\, v_{KL}\,, \tag{2.6}$$

and the complex rotational part given by

$$\mathcal{A}_{KL}(t) \;=\; M_{KL}\, e^{i\,[\Omega_{KL}(t-t_0)+\lambda_{KL}]}\,. \tag{2.7}$$

The term Φ_{KL} can be interpreted as the part of the field that is locally growing (both positively or negatively) with tendency v_{KL}. The term $\mathcal{A}_{KL}$ represents the moving part of the wave.

Fig. 2.3 shows some examples of the time evolution of selected spectral coefficients of the ALADIN forecast of the Christmas storm between 0900 UTC and 1200 UTC to formula (2.5). Each time step is represented by a small rectangle. A fit of the function (2.5)-(2.7) is superposed on each panel (solid lines)[1]. This fit quantifies the validity of the hypothesis that the evolution can be decomposed into a rotating and a linear part.

From Fig. 2.3 we see that within time intervals of a few hours (3 h in this case) and for the large scales, i.e. the scales of the storm (100 km and more), at the level of the spectral coefficients, the time evolution manifests itself as a combination of a linear trend and a rotation in the complex plane. Note that the fit is is better for larger length scales. For instance in panels (j) and (l) corresponding to wave lengths $l_{16,-3} = 175km$, and $l_{19,19} = 106km$, the fits are of lower quality.

The aim of the present paper is to test whether this behavior of the spectral coefficients can be exploited to improve the LBC temporal resolution problem. As mentioned above this will be studied in a one dimensional spectral shallow-water model on a single horizontal level. It uses velocity and geopotential as model fields and it can run on global or limited area domains. The term global domain herein describes a periodic domain where a signal that exits on one end re-enters on the opposite side. Use of the limited-area domain implies a coupling procedure on the domain edges. It is integrated with two time level semi-implicit semi-Lagrangian scheme with a second order accurate treatment of the non-linear residual [**?**].

[1] The fit was taken as the optimal estimate for the parameters in F_{KL} by minimizing the cost function

$$I\,[\Omega_{KL}, M_{KL}, \lambda_{KL}, v_{KL}, \phi_{KL}] = 12 \sum_{\alpha=0}^{n_t} \overline{(F_{KL}(t_0 + \alpha\Delta t) - c^{\alpha}_{KL})}\; (F_{KL}(t_0 + \alpha\Delta t) - c^{\alpha}_{KL})\;,$$

by a conjugate gradient method [**?**, following]]Gilbert1992. The bar denotes the complex conjugate.

A shallow-water spectral limited-area model that applies Fourier spectral representation on the model variables requires usage of time-dependent periodic LBCs [**?**]. Semi-implicit time integration and solving the Helmholtz equation in spectral space constrains the coupling procedure to be applied at the very beginning or end of the gridpoint computations [**?**]. Another solution would be to develop a simple and cheap procedure that can be applied in the spectral space. The width of the extension zone is determined by the fact that the extended boundary fields should be well represented by the used truncation [**?**]. The non-linear terms of the model equations are computed without aliasing if the number of grid points in the whole integration area is chosen so that $N_x > 3M + 1$ where M is the truncation wavenumber. Weak numerical diffusion is applied in spectral space at the end of the time step to alleviate accumulation of energy at the smallest scales due to spectral blocking.

The large scale model is a periodic low resolution model that provides LBCs and will be referred to as the global model henceforth. In the tests, two sets of model runs are performed, the global and the LAM. The global model and LAM are using the same initial conditions that consist of a Gaussian shape depression that propagates from west to east with constant speed through the whole domain.

The global model is run on 200 grid points with Δx=40km and the truncation wavenumber 66. The LAM run is on 200 grid points 11 of them are the extension zone on east and the 8 points on the eastern and western edge of the remaining 189 points are the relaxation zones. The horizontal resolution of the LAM was Δx=10km and the truncation wavenumber is equal to the one used in the global model since the number of grid points is the same. Both models use the same time step of 150 seconds.

Time steps when the large scale data are available will be referred to as the coupling steps. They are separated by the coupling interval. The coupling procedure is done at each time step. It consists of spatial and temporal interpolation and the coupling scheme, e.g.. the [**?**] scheme. The large scale data are interpolated in space onto the LAM grid and then interpolated in time to be used at each LAM time step. The 3h coupling interval is 72 time steps of the LAM.

2.4 Gridpoint coupling

This section demonstrates the capability of the simple model described in the previous section, to reproduce problems associated with interpolation of LBC in time on narrow lateral zones. The flow-relaxation coupling scheme proposed by [**?**] relaxes the interior flow to the prescribed exterior flow consuming gravity wave energy and fine spatial scale potential vorticity in a narrow zone near lateral boundaries representing adequately the outgoing gravity waves as well as geostrophic flow through the boundary. This zone is called the relaxation zone and its width will be 8 grid points of the LAM domain in the following tests. On the lateral boundaries, the LAM is forced with the large scale solution. The value of the model variable in the relaxation zone (X_C) is computed from the large scale (X_{LS}) and the small scale (X_{SS}) values by

$$X_C = \alpha X_{LS} + (1-\alpha) X_{SS}\,, \tag{2.8}$$

using the relaxation coefficient α

$$\alpha = (p+1)Z^p - pZ^{p+1}\,, \tag{2.9}$$

where p is the order of the polynomial (tuning parameter), $Z = \frac{|x-x_e|}{x_c-x_e}$ is the distance of the gridpoint x from the domain edge x_e relative to the width of the coupling zone $(x_c - x_e)$. The relaxation coefficient $\alpha = 1$ in the extension zone and $\alpha = 0$ in the central zone of LAM.

The large scale solution is known only at coupling steps t_0, t_1, t_2, ... where t_0 is usually the initial time and the coupling intervals usually kept constant, e.g. in operational applications 3 hours, which is much longer than the typical time step used in operational LAM (5-10 minutes). The large scale model state X used in the relaxation zone is interpolated in time linearly:

$$X(t) = w_1 X_{t_1} + w_2 X_{t_2} \quad \text{where} \quad w_1 = \frac{t_2 - t}{t_2 - t_1} \quad \text{and} \quad w_2 = \frac{t - t_1}{t_2 - t_1}, \tag{2.10}$$

or quadratically

$$\begin{aligned} X(t) = w_1 X_{t_1} + w_2 X_{t_2} + w_3 X_{t_3} \quad \text{where} \quad w_1 &= \frac{(t_2 - t)(t_3 - t)}{(t_2 - t_1)(t_3 - t_1)} \quad , \\ w_2 = \frac{(t_1 - t)(t_3 - t)}{(t_1 - t_2)(t_3 - t_2)} \quad \text{and} \quad w_3 &= \frac{(t_1 - t)(t_2 - t)}{(t_1 - t_3)(t_2 - t_3)} \quad , \end{aligned} \tag{2.11}$$

or using the tendency of the model state [**?**]

$$X(t) = w_1 X_{t_1} + w_2 X_{t_2} - w_1 w_2 (t_2 - t_1) \left[\left(\frac{\partial X}{\partial t} \right)_{t_2} - \left(\frac{\partial X}{\partial t} \right)_{t_1} \right] \quad . \tag{2.12}$$

where w_1 and w_2 are computed as in linear interpolation scheme. Another solution can be to increase the size of the coupling zone to include the area where the depression appears at the coupling step.

We need to determine the appropriate reference simulation to be used as reference for computation of error introduced by the coupling or time interpolation scheme. The effectiveness of the boundary updating was first tested using the method of [**?**].

Test 1 The global model was run using the same horizontal resolution as the LAM, on 800 grid points with Δx=10km and the truncation wavenumber 264. The LAM was run on the same domain as usual, but coupled to the high resolution global model using the flow relaxation scheme. In the first test, output from the high resolution global model was used from every time step so interpolation in time or space was not needed.

Test 2 In the second test, the output from the high resolution global model was taken with a 3 hour interval and interpolated in time only.

Test 3 In the third test the output from the low resolution global model was used from every time step so the LBC data were interpolated in space only.

There was no difference between the global and the LAM solutions in the first test when the flow relaxation scheme was used, as was expected [**?**]. The difference between the results from the first and the second test represents the error due to the temporal interpolation procedure. The difference between results of the first and the third test represents the error due to spatial interpolation (Figure 2.4) and different global model resolutions. The results of the global model run with different spatial resolutions are different. Consequently, LAM is coupled to the different global model data and the error is large. In other words, the disturbance that enters the domain is different so the error is not only due to spatial interpolation but it is still lower than the error due to temporal interpolation. This is why the result of the third test will be used as reference in the rest of the article.

Using gridpoint coupling with large scale data available with only 3 hourly interval allows for the depression to enter the domain area almost unnoticed (Figure 2.5). When the same computational scheme is used but with new large scale data available at every LAM time step (Test 3), the disturbance is detected by the coupling scheme and further developed by the LAM (Figure 2.6a). This result represents our ideal goal of "perfect coupling" to be reached by the modified or new coupling scheme. Unfortunately, such perfect conditions of data availability are hardly ever met by LAM users, so other options are tested. Quadratic interpolation in time does not improve the results (not shown) while using the tendencies as well as values of the model variables with 3 hourly interval does improve the results (Figure 2.6b) but

unfortunately, this is still far from the desired ideal. When the LAM domain was shifted so that the depression minimum enters the domain at the moment when the large scale data are available, the depression was recognized, but its shape was distorted by the time interpolation of the large scale data (Figure 2.7a). Another simple geometry solution would be to increase the size of the coupling zone. When its width was five-fold its usual (Figure 2.7b) the depression was recognized, but it also produced some spurious phenomena when the disturbance was leaving the domain.

Figure 2.8 shows the evolution of the model error due to the time-interpolation procedure [**?**] of the wind variable using Test 3 as reference. The error increases as the disturbance enters the domain, between 72 and 144 time steps and decreases when it leaves the LAM domain, between 216 and 288 time steps. These last two results show that there is an error inherent in the temporal interpolation and/or the coupling scheme since it misinterprets or spoils the features that enter the domain giving more incentive for finding an alternative coupling or more suitable time interpolation scheme.

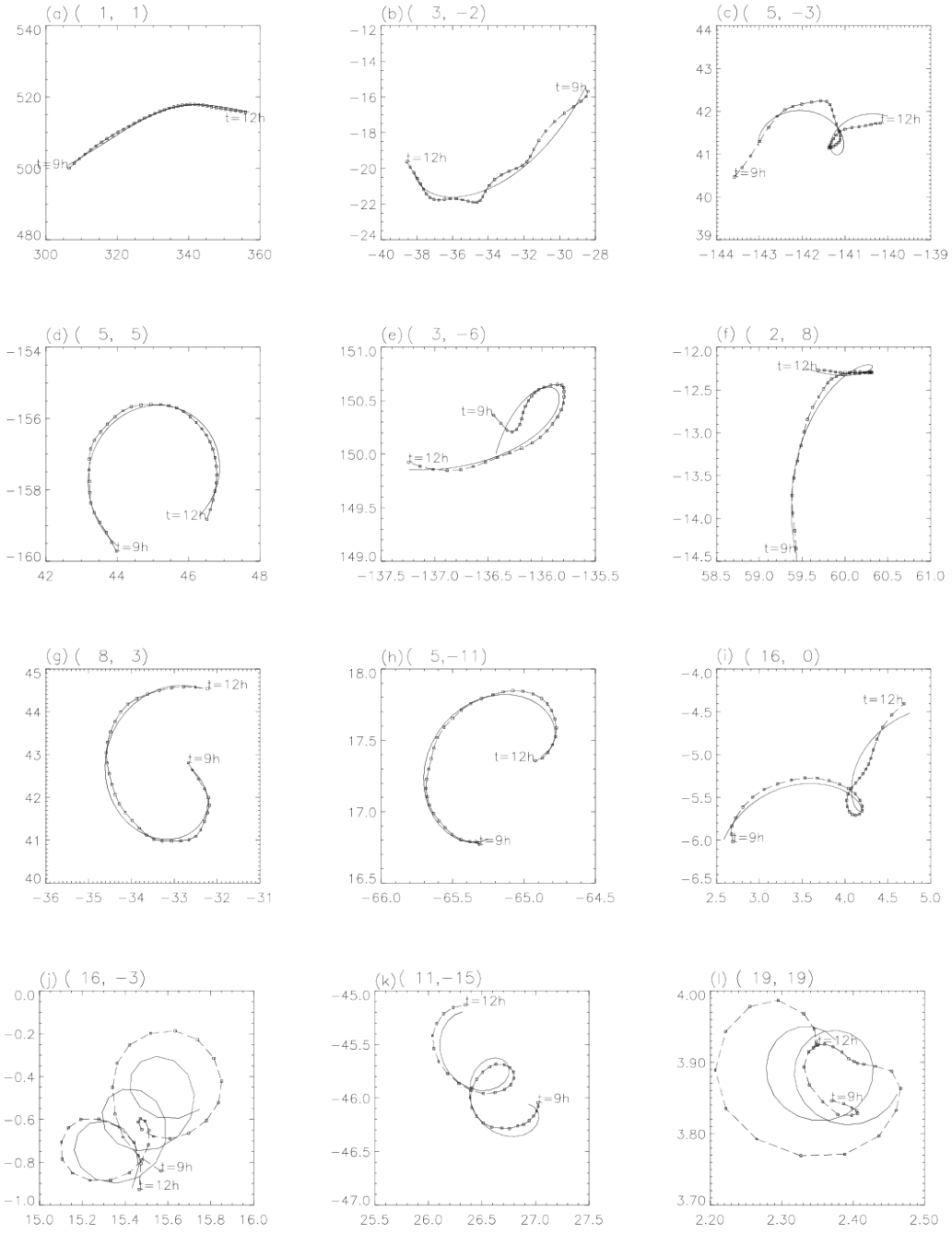

Figure 2.3: Fits (solid lines) of selected spectral coefficients of the ALADIN forecast of the Christmas storm between $09h$ and $12h$ forecast range, compared to the forecast data (a) $c^{\alpha}_{1,1}$, (b) $c^{\alpha}_{3,-2}$, (c) $c^{\alpha}_{5,-3}$, (d) $c^{\alpha}_{5,5}$, (e) $c^{\alpha}_{3,-6}$, (f) $c^{\alpha}_{2,8}$, (g) $c^{\alpha}_{8,3}$, (h) $c^{\alpha}_{5,-11}$, (i) $c^{\alpha}_{16,0}$, (j) $c^{\alpha}_{16,-3}$, (k) $c^{\alpha}_{11,-15}$, (l) $c^{\alpha}_{19,19}$ (points). The x and y axis indicate the real and imaginary part respectively (in Pa).

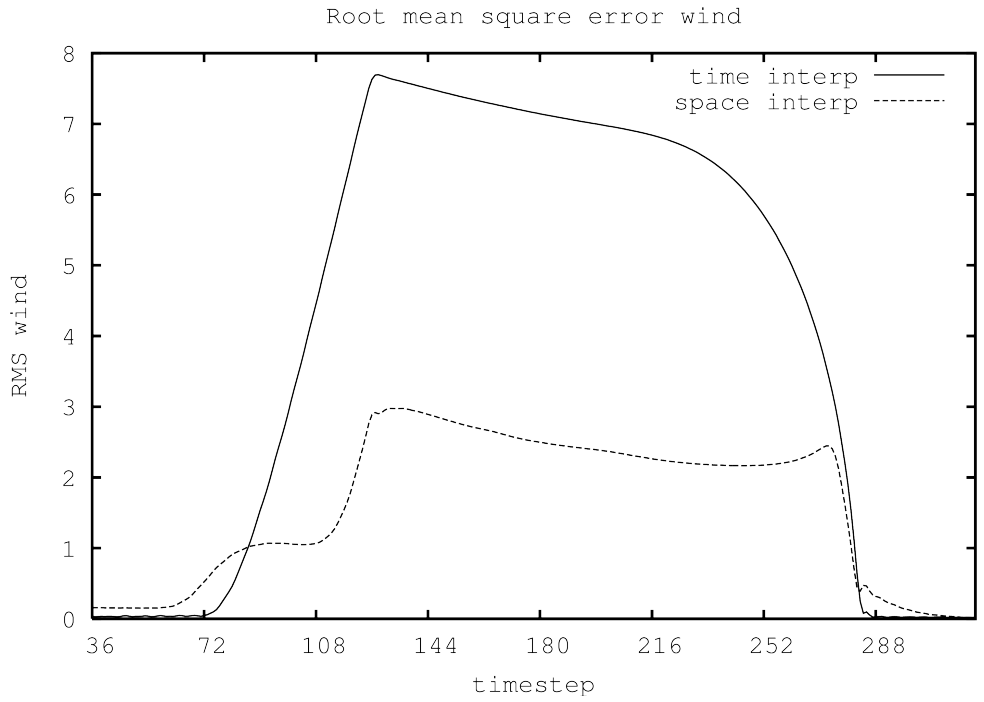

Figure 2.4: Root mean square error of wind variable computed over the LAM domain using the LAM coupled to high resolution global model as reference, for LAM coupled to high resolution global data with 3h interval (line) and coupled to low resolution global data from every time step (dashed).

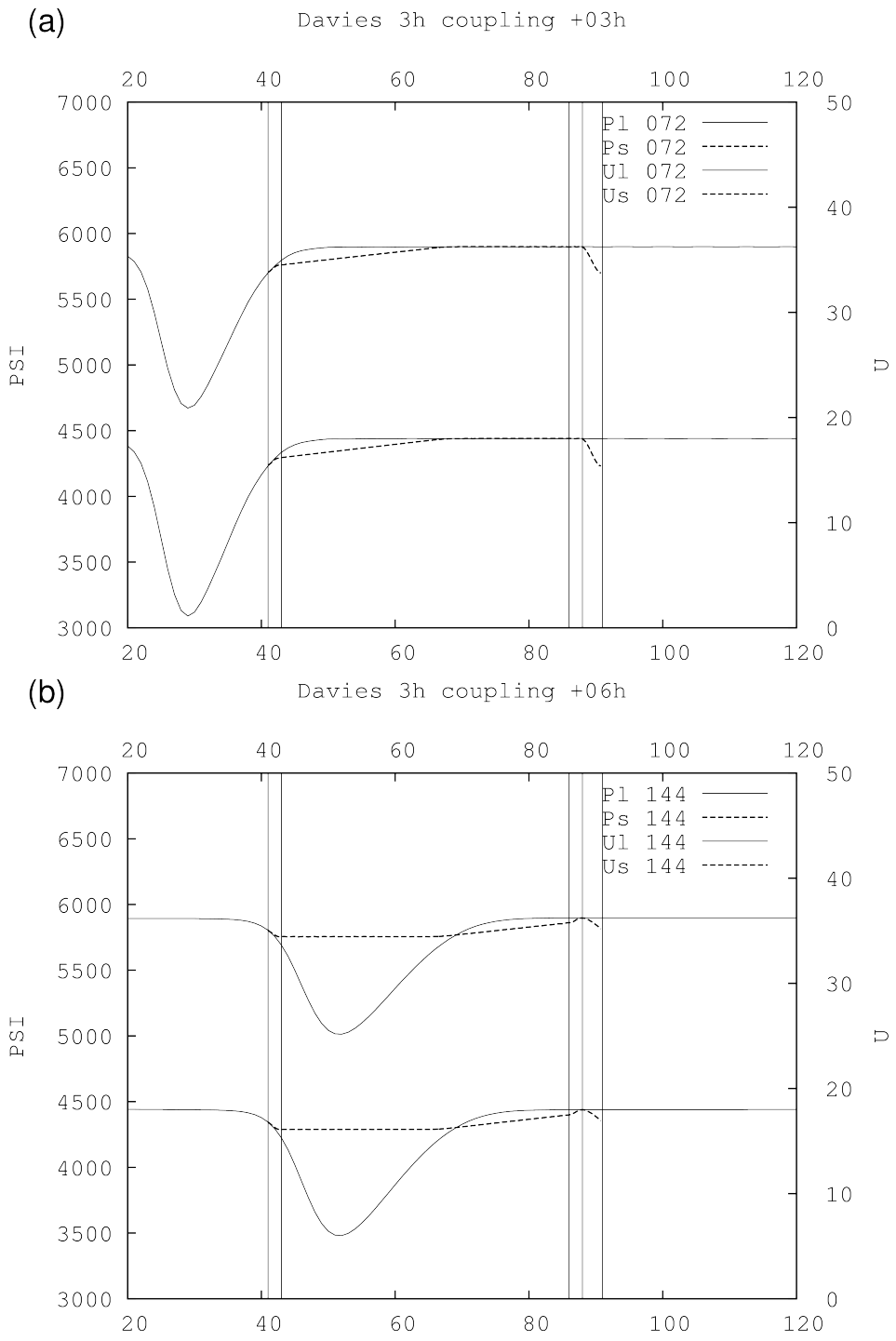

Figure 2.5: Results for coupling using Davies scheme with 3 hour interval between input large scale data, before the depression enters the domain, 3 hour forecast (a) and after, 6 hour forecast (b). Global model (full line) and limited area model (dashed) results for geopotential are shown above the results for the wind variable. Vertical lines are, from left to right, left edge of the LAM domain, right edge of the left coupling zone, left edge of the right coupling zone, right edge of the right coupling zone (also left edge of the extension zone) and the right edge of the LAM domain.

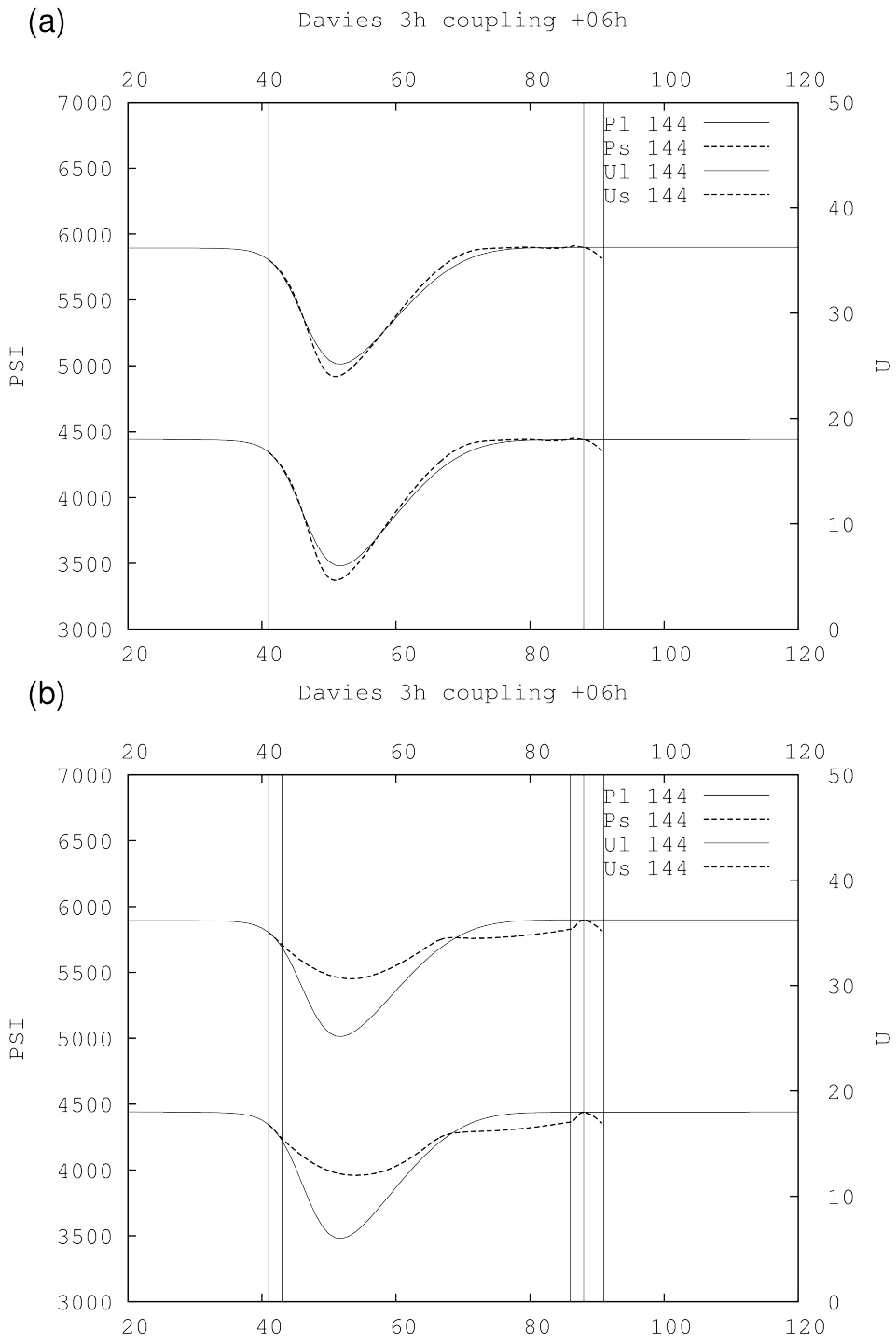

Figure 2.6: Results for coupling using Davies scheme with 1 time-step interval between input large scale data (a) and with 3 hour interval between input large scale data but using tendencies of the large scale fields for coupling (b). Both are 6 hour forecasts. Lines have the same meaning as in Figure 2.5

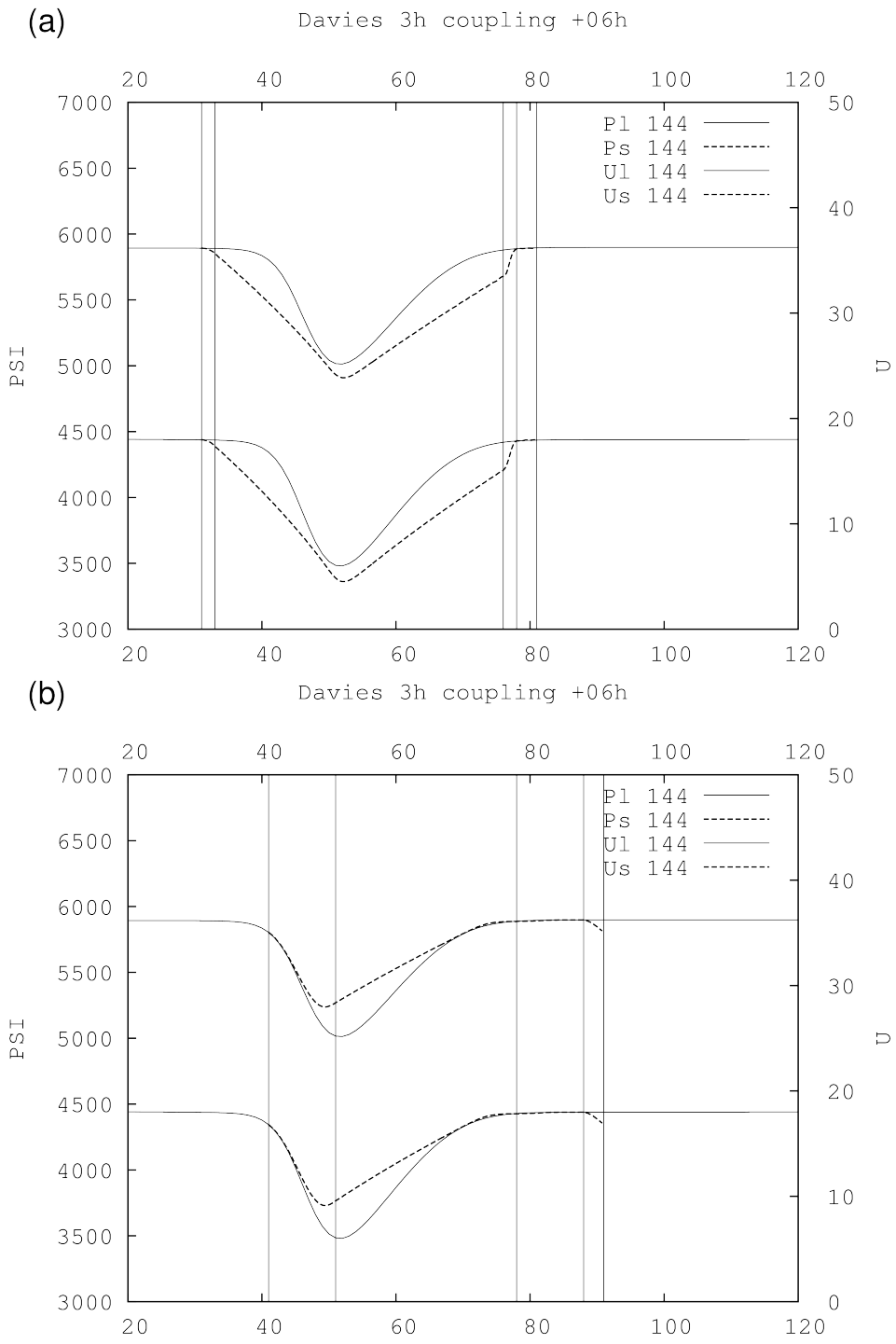

Figure 2.7: Results for coupling using Davies scheme with 3 hour interval between input large scale data and LAM domain shifted so that the depression enters the domain at the time large scale data are known (a) and when the coupling zone is increased 5 times: using 40 instead of 8 points (b). Lines have the same meaning as in Figure 2.5

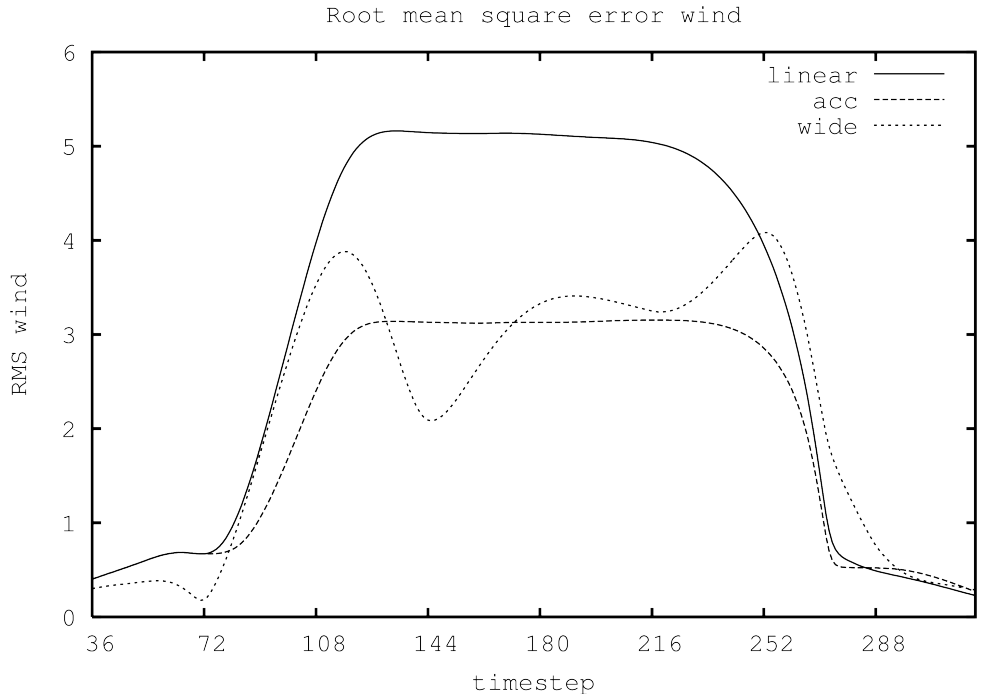

Figure 2.8: Root mean square error of wind variable computed over the LAM domain using the LAM coupled to low resolution global model for each time step as reference, for LAM coupled using flow relaxation scheme to low resolution global data with 3h interval interpolated linearly in time (line), using acceleration (long dash) and wider coupling area (short dash).

2.5 Spectral coupling

As mentioned in the introduction, the coupling of LAM to a global model can be achieved using a procedure similar to spectral nudging that will be referred to as spectral coupling. This coupling is done ovet the whole domain area, not onls the boundaries. The spectral coupling scheme was built using similar mechanism as the flow-relaxation scheme. Small wavenumber state (long waves) is taken from the large scale, large wavenumber state (short waves) is taken from LAM with a smooth functional transition in between. In other words, the large scale solution is spectrally filtered and blended with the LAM solution. The coupling scheme was developed on a basis of a spectral model used with a Fourier transform. The details are described in the following subsection.

2.5.1 The coupling method

For wave numbers lower than some threshold k_0 we take spectral coefficients from the large-scale model. For the wave numbers larger than another threshold value k_1, the spectral coefficients are taken from the LAM. The spectral coefficients for wave numbers between k_0 and k_1 are computed as

$$SP_C = \alpha SP_{LS} + (1-\alpha)SP_{SS}\,, \tag{2.13}$$

where the subscript C denotes the coupled values, LS denotes the values from large scale model and SS denotes values from small scale model. In analogy with the flow-relaxation scheme, the dependency of the α coefficient on the wave number k can be linear

$$\alpha = \frac{k_1 - k}{k_1 - k_0}\,, \tag{2.14}$$

or have a polynomial dependence on k

$$\alpha = (p+1)z^p - pz^{p+1} \qquad for \qquad p > 0 \tag{2.15}$$

$$\alpha = 1 - (-p+1)(1-z)^{-p} - pz^{-p+1} \qquad for \qquad p < 0 \tag{2.16}$$

where $z = \frac{k_1-k}{k_1-k_0}$ is the relative distance of the wave number k from the small scale wave number k_1 and p is the order of the polynomial. The boundary wave numbers (k_0 and k_1) are tunable parameters, set according to the model resolutions and the size of the LAM domain. The choice of $k_0 = 2$ and $k_1 = 8$ address the need to describe the scales that are too large to be periodic in LAM [**?**] using lateral boundary data. The polynomial dependence of α on wave number did not bring much improvement over the linear one in the

tests using the simple one dimensional model, so the linear dependence will be kept in the following experiments.

The spectral coupling scheme is scale selective, as the large scales are dominated by the spectra of the large scale model and only small scales are dominated by the spectra of the LAM. Its advantage is that the large scale solution is forced to LAM on the whole domain area. Unfortunately, spectral coupling scheme alone cannot eliminate spurious wave propagation from the lateral boundaries inward. Due to biperiodization, a necessity of a spectral LAM, without the gridpoint flow relaxation at the boundaries, all the waves that exit on one side of the domain freely enter on the opposite side. This is why we still need to use the gridpoint flow-relaxation scheme simultaneously to provide the damping on the domain edges. In other words, both coupling methods are combined. The relaxation takes place at the end of the gridpoint computations simultaneously with the flow-relaxation scheme.

2.5.2 Coupling without interpolation of large scale fields in time

As shown in previous sections, time interpolation can introduce significant errors to the model results. These errors could be avoided by not doing the time interpolation at all. The large scale fields are known only at discrete time intervals. In the gridpoint coupling scheme the coupling is done every time step and the large scale fields on the boundaries are interpolated in time. Spectral coupling forces the large scale solution LAM over the whole domain and could be done only at the coupling steps, when the large scale data are available, or more often, up to every LAM time step.

First several options were tested of introducing large scale data into the LAM without being interpolated in time. The large scale spectral coefficients are inserted to the LAM and the gridpoint part of the coupling scheme is left unchanged. If the LAM solution is forced by the large scale one only at the coupling steps, the depression appears suddenly, during one time step. Such result suggests that this method is not good for a real LAM with more sophisticated dynamics and physics parameterization package.

Instead of introducing large scale data suddenly, in one time step, an attempt was made to introduce it gradually during the coupling interval, so that coupling coefficient α was multiplied by a time dependent β function

$$\beta = \left(max \left[0, \frac{1}{1 - t_s} \left(\frac{t - t_1}{t_2 - t_1} - t_s \right) \right] \right) \tag{2.17}$$

where t_s is the time when the large scale solution from the second coupling time starts to be used, t_1 is the time of the first coupling file, t_2 is the time of the second coupling file. The time t is from the coupling interval $t_1 < t < t_2$. This way the large scale data are not interpolated in time, but the data from the second coupling step are gradually introduced to the model during the coupling interval.

Unfortunately, such method leads to an unphysical solution of a false rapid generation of depression that develops in the domain, not an undisturbed transfer of a depression into the model domain. Therefore, we need to accomplish a different type of smooth transition between the coupling steps that would allow more physical representation of the model evolution on the lateral boundaries.

2.5.3 Temporal interpolation of spectral coefficients

The model uses spectral coefficients, so the first attempt was to use them in the time interpolation and avoid additional computations or transformations. The spectral coefficients of the large scale fields are interpolated in time before being used by the coupling procedure. Regarding the spectral coefficients in a realistic LAM such as the ALADIN model, this corresponds to the assumption that they evolve in time linearly according to (2.6) and that the component in (2.7) is zero. This interpolation in time can be linear, but in analogy with the gridpoint coupling procedure above, also a quadratic interpolation has been investigated and the one that uses tendencies of the spectral coefficients. We use similar formulas as the ones in Eqs. (2.11) and (2.12) for gridpoint coupling when the values of the model fields are replaced by its spectral coefficients.

Results for linear interpolation of spectral coefficients in time is shown in Figure 2.9. Instead of advection of the depression, a dipole is obtained. The depression develops and then dissolves only to develop on another position simultaneously. But even this unnatural model behavior led to improvements in the model error (see Fig. 2.10). Similar results were obtained for quadratic interpolation of spectral coefficients in time as well as when their tendencies (acceleration) were used. As shown in section 2, the time evolution of spectral coefficients is better represented with time interpolation of the linear trend and rotation in the complex plane. These can be seen as amplitude and phase of waves that constitute the field in spectral space. Since interpolation spectral coefficients in time also led to unrealistic model behavior, an attempt was made using amplitude and phase of spectral components.

2.5.4 Temporal interpolation of amplitude and phase of spectral coefficients

Amplitude and phase are first computed from the spectral components and then interpolated in time. The interpolated amplitude and phase are used to compute the large scale spectral components used for coupling at a given time step. Linear and quadratic time interpolation of amplitude and phase is done using same formulas as in gridpoint coupling schemes and acceleration is accounted for in analogous way [**?**]. This approach takes into account the fact that, in realistic LAMs such as the ALADIN model, also the phases corresponding to Eq. (2.7) evolve in time. The resulting model run showed significant improvements compared to the run when spectral coefficients were interpolated. The depression was mostly advected and the dipole problem

almost disappeared. This result encouraged searching for alternative schemes for interpolation of amplitude and phase in time.

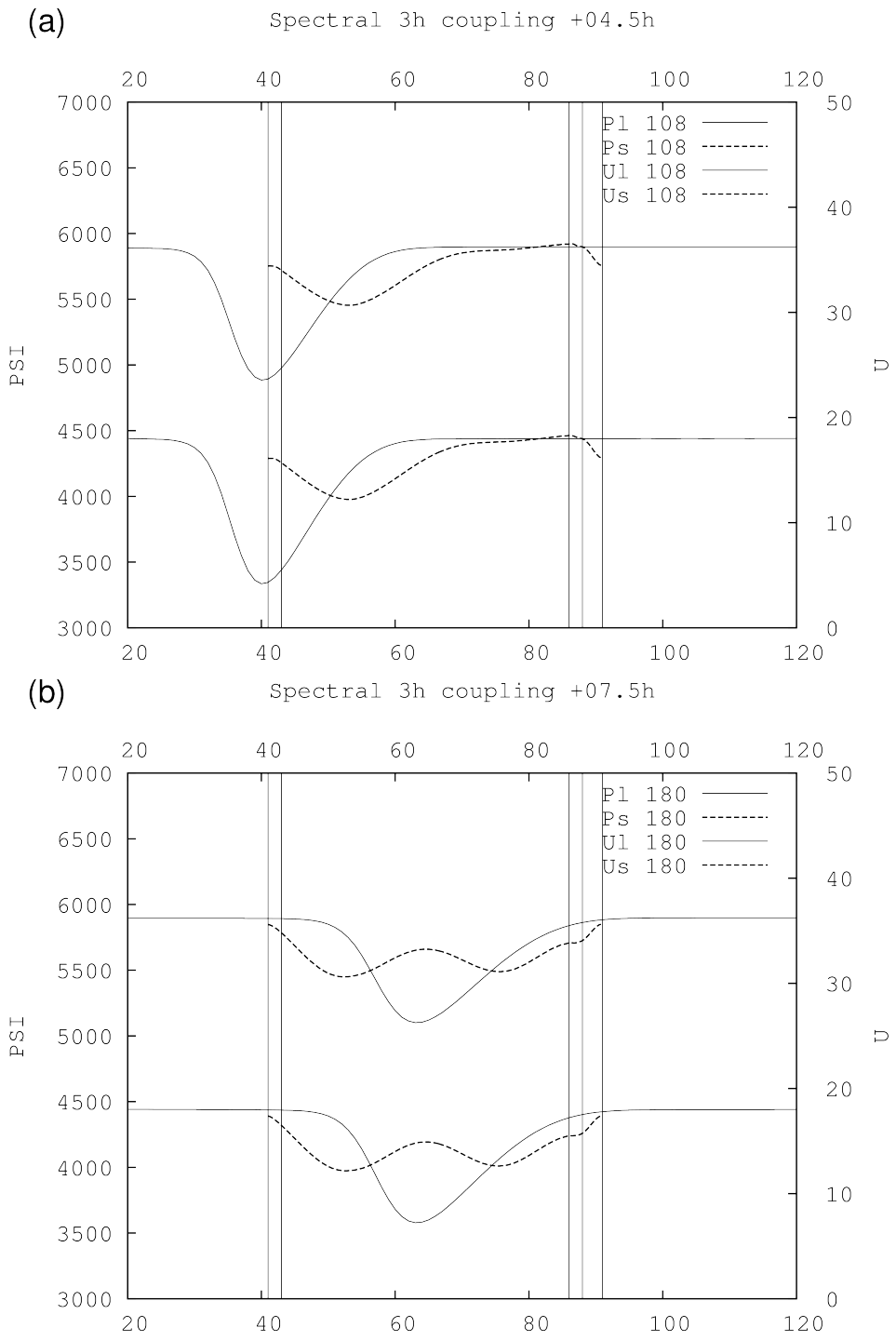

Figure 2.9: Results using spectral coupling scheme with 3 hour interval between input large scale data, when the spectral coefficients are interpolated linearly in time, after 4.5 (a) and 7.5 (b) hours. Lines have the same meaning as in Figure 2.5

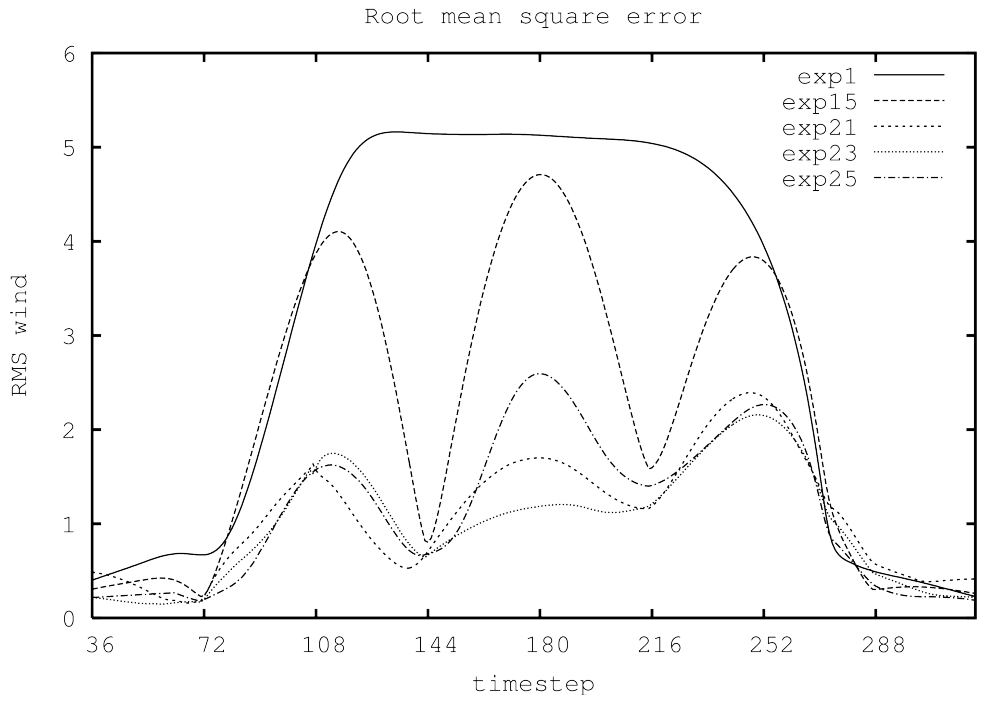

Figure 2.10: Root mean square error of wind variable computed over the LAM domain using the LAM coupled to low resolution global model for each time step as reference, for LAM coupled using flow relaxation scheme to low resolution global data with 3h interval interpolated linearly in time (full line), coupled using spectral coupling scheme when spectral coefficients are interpolated linearly in time (long dash), when the amplitude and phase of the spectral components are interpolated in time using extrapolation (short dash), integration between coupling steps (dots) or polynomial interpolation in time (dot dash).

Average of extrapolated values

An alternative time interpolating scheme has been introduced that estimates the value of the model variable X at time t by extrapolating it from the coupling steps. Assume that model variable X at one coupling step at time t_1 has known value X_1 and a time derivative $\left(\frac{\partial X}{\partial t}\right)_{t_1}$ and in the next coupling step at time t_2 has value X_2 and derivative $\left(\frac{\partial X}{\partial t}\right)_{t_2}$. The simplest way of accounting for the tendency in the interpolation scheme is to compute the forward extrapolated value from time t_1

$$X_1(t) = X_1 + \left(\frac{\partial X}{\partial t}\right)_{t_1} (t - t_1) \tag{2.18}$$

and backward extrapolated value from time t_2

$$X_2(t) = X_2 + \left(\frac{\partial X}{\partial t}\right)_{t_2} (t - t_2)\,, \tag{2.19}$$

and finally compute their weighted average

$$X(t) = w_1 X_1(t) + w_2 X_2(t), \tag{2.20}$$

where w_1 and w_2 are the same as for the linear interpolation. Usage of this interpolating scheme allows the depression to smoothly enter the domain, to be advected through it and exit (Figure 2.11). Unfortunately, there are a few spurious waves generated on top of the simulated depression that spoil the solution slightly. Another drawback is that the LAM contribution to the resulting model evolution is suppressed by the spectral nudging of the spectral components towards the large scale solution. In other words, the LAM does not bring useful contribution to the evolution of the model variables or this contribution is hidden with spurious waves that are consequence of the temporal interpolation of the large scale fields.

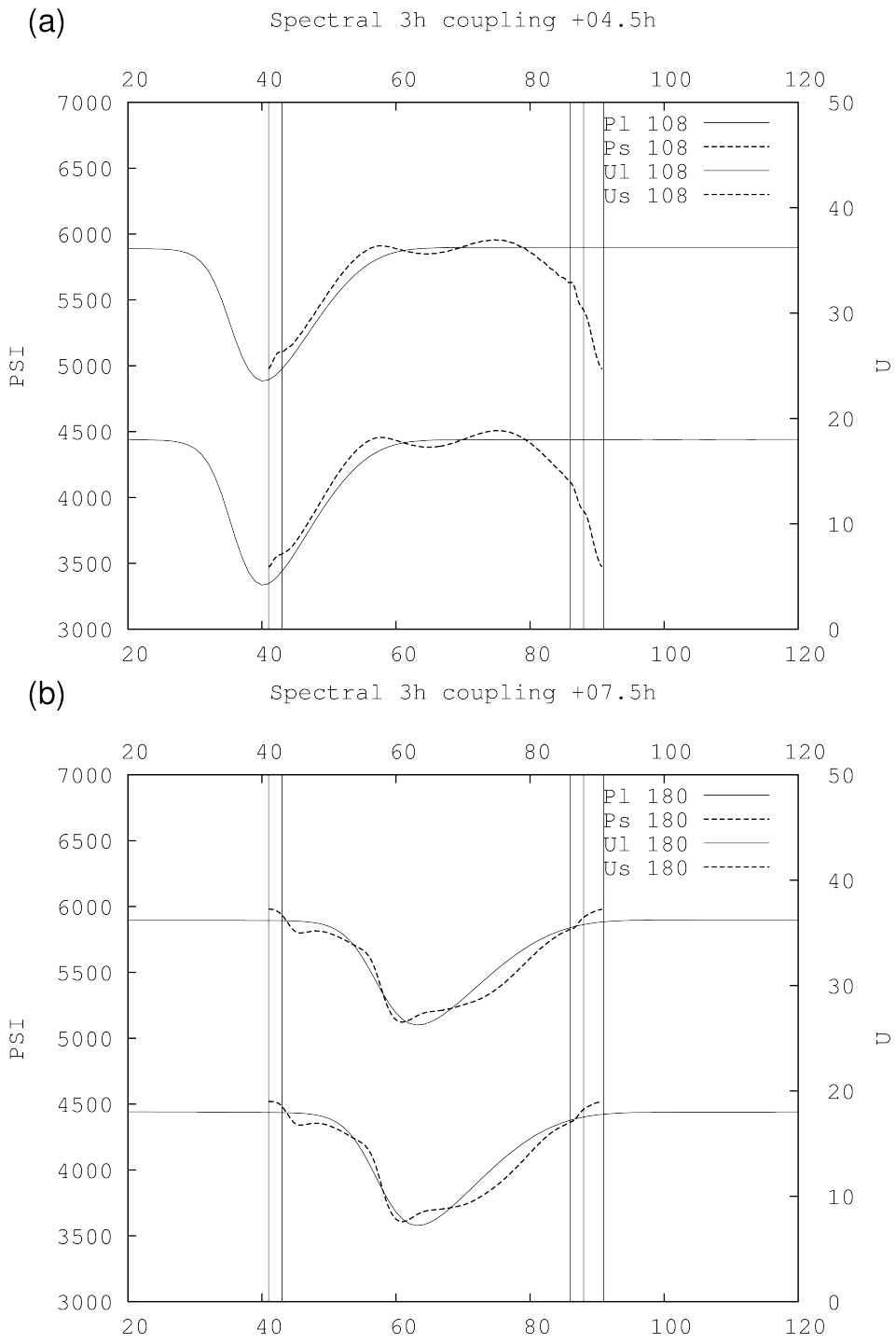

Figure 2.11: Results using spectral coupling scheme with 3 hour interval between input large scale data, when amplitude and phase are interpolated in time using the extrapolated values after 4.5 (a) and 7.5 (b) hours. Lines have the same meaning as in Figure 2.5

Integrated weighted tendencies

Instead of using fixed value for the tendency for the whole $(t-t_1)$ or (t_2-t) period, we can use a weighted average of the two tendencies at each time step and then compute the integral from t_1 to t or from t to t_2 respectively.

The value of the model variable X at time t can be estimated by forward integration of the following expression

$$X_1(t) = X_1 + \int_{t_1}^{t} \left(w_1 \left(\frac{\partial X}{\partial t} \right)_{t_1} + w_2 \left(\frac{\partial X}{\partial t} \right)_{t_2} \right) dt \,, \tag{2.21}$$

where $w_1 = \frac{t_2-t}{t_2-t_1}$ and $w_2 = \frac{t-t_1}{t_2-t_1}$ are functions of time t. The obtained function of time is

$$X_1(t) = X_1 + \left(\frac{\partial X}{\partial t} \right)_{t_1} (t-t_1) + \frac{1}{2} \left(\left(\frac{\partial X}{\partial t} \right)_{t_2} - \left(\frac{\partial X}{\partial t} \right)_{t_1} \right) \frac{(t-t_1)^2}{t_2-t_1} \tag{2.22}$$

or alternatively, a similar expression can be obtained when integrating from time t_2 backward

$$X_2(t) = X_2 - \int_{t}^{t_2} \left(w_1 \left(\frac{\partial X}{\partial t} \right)_{t_1} + w_2 \left(\frac{\partial X}{\partial t} \right)_{t_2} \right) dt \,, \tag{2.23}$$

yielding alternative function of time

$$X_2(t) = X_2 - \left(\frac{\partial X}{\partial t} \right)_{t_2} (t_2-t) + \frac{1}{2} \left(\left(\frac{\partial X}{\partial t} \right)_{t_2} - \left(\frac{\partial X}{\partial t} \right)_{t_1} \right) \frac{(t_2-t)^2}{t_2-t_1}. \tag{2.24}$$

The final interpolation function is the linear combination of the two

$$X(t) = w_1 X_1(t) + w_2 X_2(t) \,. \tag{2.25}$$

This interpolation scheme generates far less spurious waves (Figure 2.12) and apparently there is some benefit of the higher resolution LAM run since it contributes to the evolution of the disturbance.

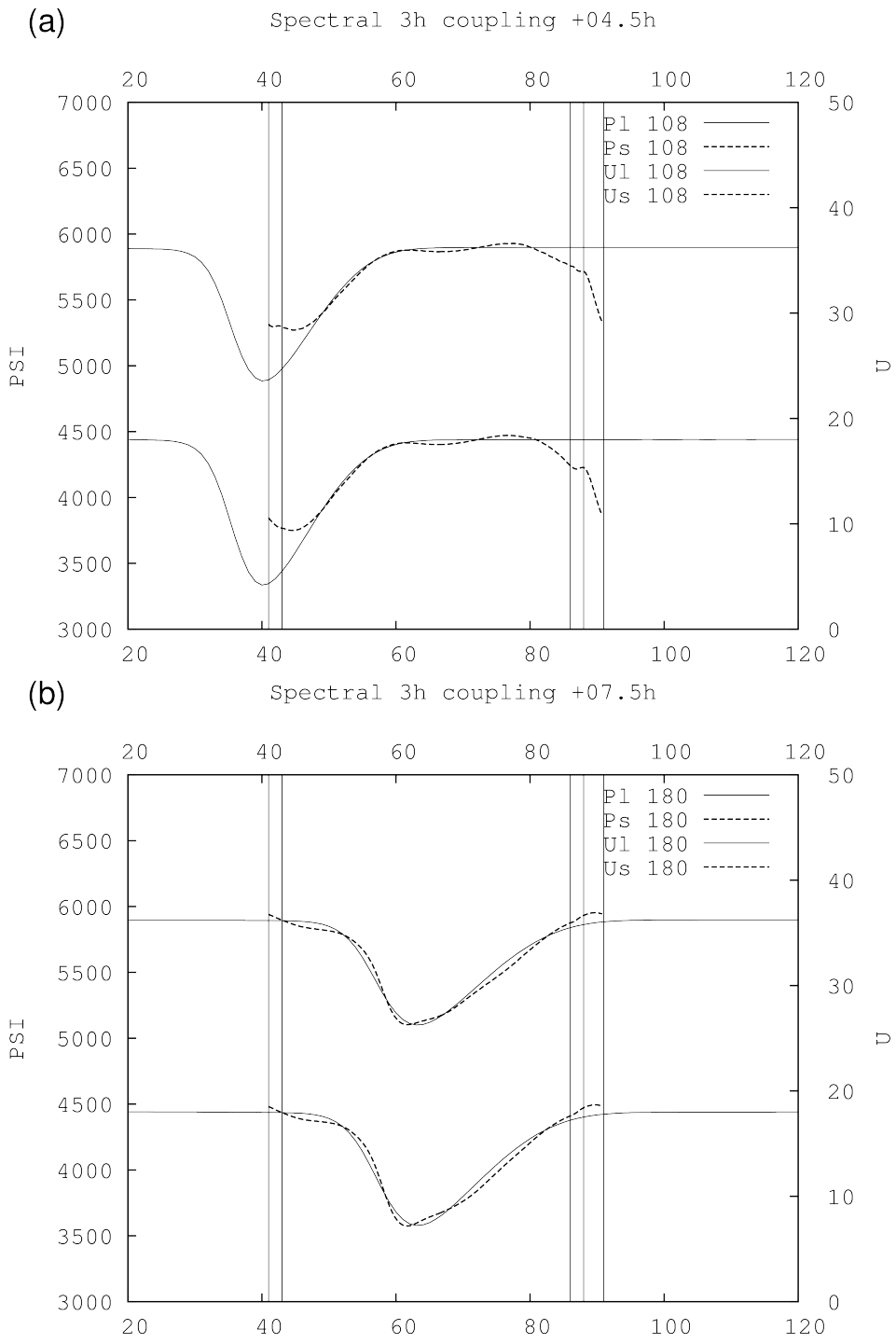

Figure 2.12: Results using spectral coupling scheme with 3 hour interval between input large scale data, when amplitude and phase are interpolated in time using the integrated values after 4.5 (a) and 7.5 (b) hours. Lines have the same meaning as in Figure 2.5

Polynomial interpolation

Another interpolation function can be computed using the values of the model variable X and its derivative at times t_1 and t_2 to evaluate coefficients in a 3rd order polynomial. First assume a polynomial dependence of the variable X in time,

$$X(t) = a + bt + ct^2 + dt^3\,, \tag{2.26}$$

and compute the coefficients assuming $t_1 = 0$ for simplicity

$$\begin{aligned}
a &= X(t=0) = X_1\,,\\
b &= \left(\frac{dX}{dt}\right)_{t=0} \left(\frac{\partial X}{\partial t}\right)_{t_1}\,,\\
c &= \frac{3}{t_2^2}\left[X_2 - X_1 - \frac{1}{3}\left(2\left(\frac{\partial X}{\partial t}\right)_{t_1} + \left(\frac{\partial X}{\partial t}\right)_{t_2}\right) t_2\right]\,,\\
d &= -\frac{2}{t_2^3}\left[X_2 - X_1 - \left(\left(\frac{\partial X}{\partial t}\right)_{t_1} + \left(\frac{\partial X}{\partial t}\right)_{t_2}\right) t_2\right]\,.
\end{aligned} \tag{2.27}$$

This interpolation scheme also allows for the depression to smoothly enter the domain, but unfortunately it also amplifies several wave components more than it should so spurious waves appear in the LAM solution (figure not shown, results qualitatively similar to those in Figure 2.11).

The spectral coupling procedure using temporal interpolation of amplitude and phase instead of spectral coefficients has reproduced the model evolution in more physical way yielding results that are similar to the test with gridpoint coupling using large scale data from each time step - the "perfect coupling" test (Figure 2.6a). The spectral coupling alone allows for waves to re-enter the domain upon exiting on the opposite side due to biperiodization of the large scale fields. Therefore it still requires simultaneous usage of the gridpoint coupling procedure on the domain edges to filter the waves that would otherwise re-enter the domain.

The model error evolution (Figure 2.10) shows the minimum values at coupling steps and maxima in the time between, when the error of the interpolation in time is largest. This is consistent with results from [**?**] who found largest errors in the boundary zone near the midpoint of the LBC update cycle. The results suggest that integrated weighted tendencies give the least spurious waves while allowing for the disturbance to enter and leave the LAM domain.

Unfortunately, the temporal interpolation scheme in combination with the spectral coupling procedure and biperiodization might generate spurious waves that could spoil the solution or mask the LAM contribution to the

model evolution. It is also possible that these spurious waves are partly a consequence of double coupling on the domain edges where the spectral coupling procedure could push the model fields in a different way than the gridpoint procedure. Therefore another alternative is sought in the next section, that could potentially allow for physical evolution of LBC conditions and enable evolution of the LAM solution in the central part of the domain undisturbed by the spectral nudging toward the large scale data.

2.6 Gridpoint coupling using amplitude and phase angle interpolation in time

The large scale model state X_{LS} is transformed from gridpoint to the spectral space, and the spectral coefficients are obtained. Then the amplitude and the phase angle of the complex spectral coefficients are computed and interpolated in time using the same procedures as when doing the spectral coupling. The time interpolated amplitude and phase angle are used to compute the time interpolated spectral coefficients which are transformed back from spectral to gridpoint space. This way we obtain the large scale fields used for gridpoint coupling.

The time interpolation of amplitude and phase can also be linear or quadratic, use acceleration, tendencies for integral or polynomial interpolation. When the amplitude and phase are interpolated linearly in time, the simulated depression is significantly weaker than with the perfect coupling scheme, but recognized. Unfortunately, when the depression leaves the domain, it is followed by a strong false positive signal (not shown). Results using quadratic coupling are very similar to the linear one. When the acceleration of amplitude and phase is used, the simulated depression is stronger and the false anticyclone is reduced. Using the average of extrapolated values gives satisfactory depth of the depression but the amplitude of few short modes is a bit too strong (Figure 2.13). Other results using tendencies of the model fields, either integrated between coupling steps or using polynomial interpolation give similar results as the simplest case shown in Figure 2.13. The depression enters the domain, although it is less deep than in the large scale model. But since this scheme relaxes the LAM solution to the large scale one only in the narrow area close to the domain edge, the LAM can contribute to the development of the disturbance. Unfortunately, the other benefit of the gridpoint coupling is lost since the longest modes also re-enter the domain, although much weaker. This is a consequence of the biperiodization of the large scale fields. The evolution of the model error (Figure 2.14) shows an increase after the depression leaves the domain, due to these excessive waves.

2.7 Disucussion and conclusions

The present paper aims to improve the LBC temporal resolution problem. A LAM that uses LBC data from a storage utility or remote center usually has the data available with a coupling interval of several hours. LBC data are interpolated in time and used in LAM each time-step of several minutes.

The features with time-scales shorter than the coupling interval are corrupted or even removed by the time-interpolation procedure. The problem has encouraged the research on the coupling procedure that would enable a better representation of such features using the available LBC data.

It was shown (Figure 2.1d) that linear interpolation of LBC within 3h interval distorts the model fields. The interpolation procedure created two cyclones instead of one. The time evolution of the large scale model fields is poorly represented by the time-interpolated fields on the domain edges. The evolution of model fields in time is better represented by a linear trend and a rotation of spectral coefficients in the complex plane (Figure 2.4). This data obtained for a realistic 3D model served as inspiration to improve the temporal interpolation, in particular of the spectral coefficients. And these alternatives for the commonly used linear interpolation were tested using a simple 1D model. The tests reveal what error can be expected when using the different coupling and time-interpolation schemes.

Gridpoint coupling using standard Davies scheme on a narrow area close to the edges of the LAM domain with a coupling interval of several hours misses a signal that enters the domain. Two possible alternatives to the standard Davies coupling are presented in the framework of a simple one-dimensional model. The first one does the coupling in the spectral space. This method is also known as spectral nudging and has shown benefits in other models (eg. [**?**]). The second one only interpolates the large scale fields in time in spectral space but does the coupling in gridpoint space. Both of them are able to represent the missed signal in the LBC, but the second one could be the first step further from the "standard" gridpoint coupling using fields interpolated linearly in time.

Usage of the spectral coupling alone supports spurious waves that could re-enter the domain as a consequence of biperiodization. These waves can be filtered by the gridpoint coupling scheme, as was done in previous studies when the boundary relaxation scheme was found necessary for LBC noise removal [**?**].

Time interpolation in spectral space improves the representation of fast small-scale disturbances in LBC data. LBC coupling scheme can benefit from the boundary relaxation scheme used in combination with the improved time-interpolation. Both schemes could be used either always or they could be applied only when the monitoring procedure proposed by [**?**] detects that some signal has entered the LAM domain without being properly sampled by the standard 3-h linear temporal interpolation.

The original idea of the dipole problem and the investigation of the cure by the phase-angle interpolation was suggested to us by Jean-François Geleyn. This work benefited from numerous useful discussions with him and Gabor

Radnóti. The authors thank the two anonymous reviewers. The manuscript was very much improved by their many pertinent remarks and suggestions.

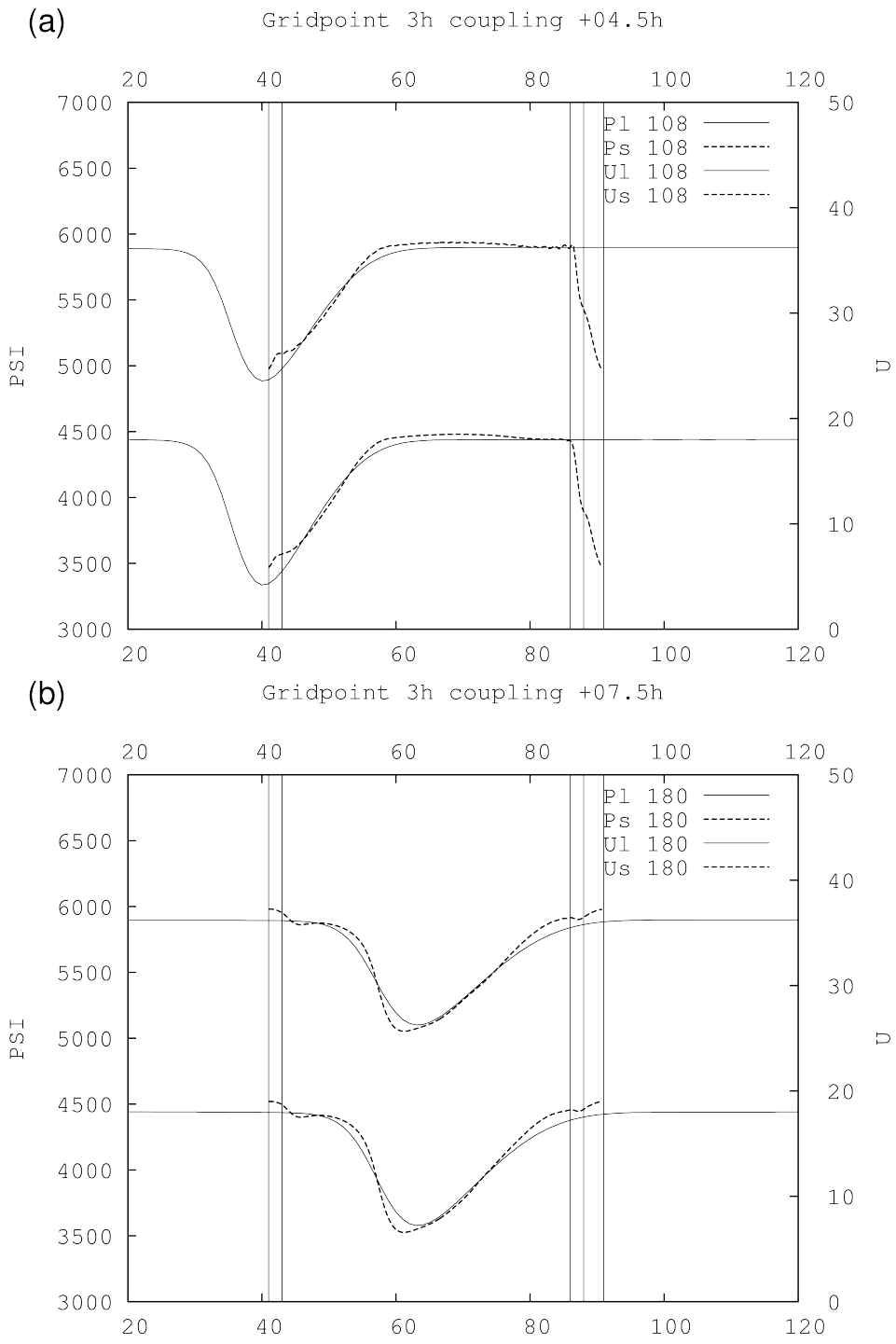

Figure 2.13: Results using spectral coupling scheme with 3 hour interval between input large scale data, when amplitude and phase are interpolated in time using the extrapolated values but coupled in gridpoint space only in the narrow area close to the domain boundary, after 4.5 (a) and 7.5 (b) hours. Lines have the same meaning as in Figure 2.5

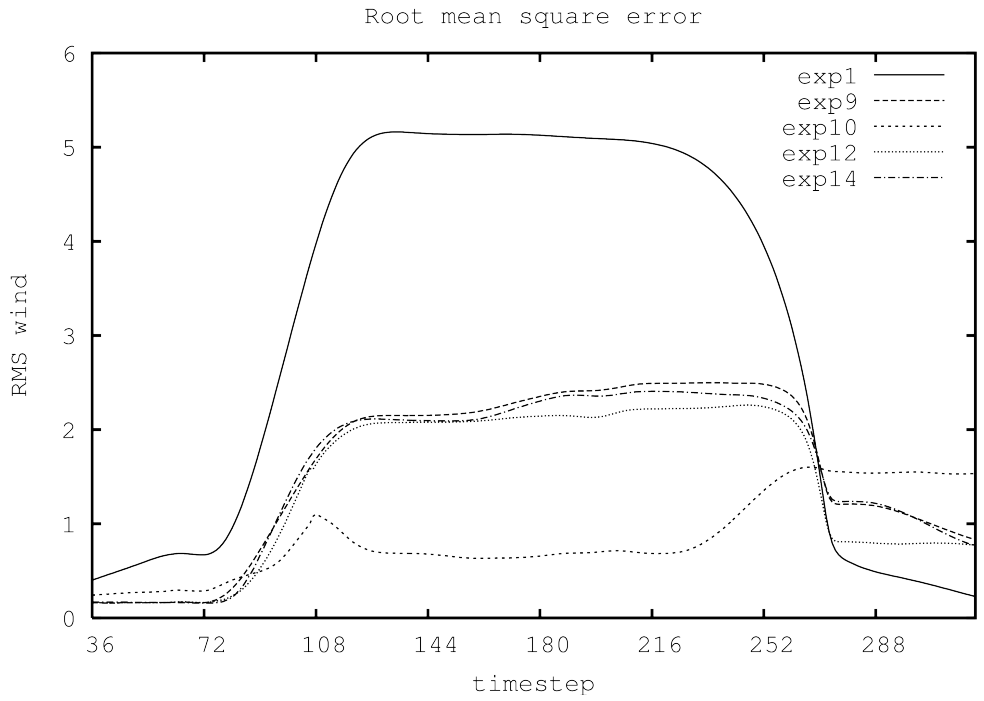

Figure 2.14: Root mean square error of wind variable computed over the LAM domain using the LAM coupled to low resolution global model for each time step as reference, for LAM coupled using flow relaxation scheme to low resolution global data with 3h interval interpolated linearly in time (full line), coupled in gridpoint space but the large scale data are interpolated in spectral space: when the amplitude and phase of the spectral components are interpolated in time using amplitude (long dash) extrapolation (short dash), integration between coupling steps (dots) or polynomial interpolation in time (dot dash).

Bibliography

[ALADIN International Team(1997)] ALADIN International Team:, The ALADIN project: Mesoscale modelling seen as a basic tool for weather forecasting and atmospheric research, WMO Bull., 46, 317–324, 1997.

[Alpert et al.(1990)] Alpert, P., Neeman, B.U., and Y. Shay-El, Y.; Inter-monthly variability of cyclone tracks in the Mediterranean, J. Climate, 3, 1474–1478, 1990.

[Boyd(2005)] Boyd, J.P.: Limited-Area Fourier Spectral Models and Data Analysis Schemes: Windows, Fourier Extension, Davies Relaxation, and All That. Mon. Wea. Rev., 133, 2030–2042, 2005.

[Branković et al.(2007)] Branković, Č., Matjačić, B., Ivatek-Šahdan, S., and Buizza, R.: Dynamical downscaling of ECMWF EPS forecasts applied to cases of severe weather in Croatia, ECMWF RD Technical Memorandum, No. 507, 38 pp., 2007.

[Branković et al.(2008)] Branković, Č., Matjačić, B., Ivatek-Šahdan, S., and Buizza, R.: Downscaling of ECMWF Ensemble Forecasts for Cases of Severe Weather: Ensemble Statistics and Cluster Analysis, Mon. Wea. Rev., 136, 3323–3342, 2008.

[Brožkova et al.(2001)] Brožkova, R., Klarić, D., Ivatek-Šahdan, S., Geleyn, J.-F., Casse, V., Široká, M., Rádnoti, G., Janoušek, M., Stadlbacher, K., and Seidl, H.: DFI Blending, an alternative tool for preparation of the initial conditions for LAM, PWRP Report Series No. 31, WMO-TD, No. 1064, 2001.

[Campinis at al.(2000)] Campinis, J., Genoves, A., Jansa, A., Guijarro, J.A., and Ramis, C.: A catalogue and a classification of surface cyclones for the Western Mediterranean, Int. J. Climatol., 20, 969–984, 2000.

[Cassou and Terray(2001)] Cassou, C., and Terray, L.: Oceanic forcing of the wintertime low-frequency atmospheric variability in the north atlantic

european sector: a study with the arpege model, J. Climate, 14, 4266–4291, doi: http://dx.doi.org/10.1175/1520-0442(2001)014, 2001.

[Courtier and Geleyn(1988)] Courtier, P., and Geleyn, J.-F.: A global numerical weather prediction model with variable resolution: application to the shallow water equations. Quart. J. Roy. Meteor. Soc., 114, 1321–1246, 1988.

[Davies(1976)] Davies, H.C.: A lateral boundary formulation for multi-level prediction models. Q. J. R. Meteorol. Soc., 102, 405–418, 1976.

[Davies(1983)] Davies, H.C.: Limitations of some common lateral boundary schemes used in regional NWP models. Mon. Wea. Rev., 111, 1002–1012, 1983.

[Davies(2014)] Davies, T.: Lateral boundary conditions for limited area models. *Q. J. R. Meteorol. Soc.*, 140: 185–196, 2014.

[Dee et al.(2011)] Dee, D. P., Uppala, S.M., Simmons, A.J., Berrisford, P., Poli, P., Kobayashi, S., Andrae, U., Balmaseda, M.A., Balsamo, G., Bauer, P., Bechtold, P., Beljaars, A.C.M., van de Berg, L., Bidlot, J., Bormann, N., Delsol, C., Dragani, R., Fuentes, M., Geer, A.J., Haimberger, L., Healy, S.B., Hersbach, H., Hólm, E.V., Isaksen, L., Kàllberg, P., Köhler, M., Matricardi, M., McNally, A.P., Monge-Sanz, B.M., Morcrette, J.-J., Park, B.-K., Peubey, C., de Rosnay, P., Tavolato, C., Thépaut, J.-N., and Vitart, F.: The ERA-Interim reanalysis: configuration and performance of the data assimilation system. *Q. J. R. Meteorol. Soc.*, 137, 553–597. doi: 10.1002/qj.828, 2011.

[Degrauwe et al.(2012)] Degrauwe, D., Caluwaerts, S., Voitus, F., Hamdi, R., and Termonia, P.: Application of Boyds Periodization and Relaxation Method in a Spectral Atmospheric Limited Area Model. Part II: Accuracy Analysis and Detailed Study of the Operational Impact. Mon. Wea. Rev., 140, 3149–3162, 2012.

[Denis et al.(2002)] Denis, B., Laprise, R., Caya, D. and Cŏté, J.: Downscaling ability of one-way nested regional climate models: the big-brother experiment. Climate Dynamics, 18, 627–646, 2002.

[Denis et al.(2003)] Denis, B., Laprise, R. and Caya, D.: Sensitivity of a regional climate model to the resolution of the lateral boundary conditions. Climate Dynamics, Climate Dynamics, 20, 107–126, 2003.

[De Troch et al.(2013)] De Troch, R., Hamdi, R., Van de Vyver, H., Geleyn, J.-F., and Termonia, P.: Multiscale Performance of the ALARO-0 Model for Simulating Extreme Summer Precipitation Climatology in Belgium. J. Climate, 26, 8895–8915, 2013.

[Doswell et al.(1996)] Doswell, C.A., Brooks, H.E., and Maddox, R.A.: Flash flood forecasting: An ingredients-based methodology. *Wea. Forecasting*, 11, 560–581, 1996.

[Gospodinov et al.(2001)] Gospodinov I, Spiridonov V, Geleyn J-F. 2001. Second order accuracy of two-time-level semi-Lagrangian schemes. Quart. J. R. Met. Soc. 127 : 1017–1033. DOI:10.1002/qj.49712757317

[Hamdi et al.(2012)] Hamdi, R., Van de Vyver, H. and Termonia, P.: New cloud and microphysics parameterisation for use in high-resolution dynamical downscaling: application for summer extreme temperature over Belgium. Int. J. Climatol., 32: 2051–2065. doi: 10.1002/joc.2409, 2012.

[Hamdi et al.(2014)] Hamdi, R., Van de Vyver, H., De Troch, R. and Termonia, P.: Assessment of three dynamical urban climate downscaling methods: Brussels's future urban heat island under an A1B emission scenario. Int. J. Climatol., 34: 978–999. doi: 10.1002/joc.3734, 2014.

[Haugen and Machenhauer(1993)] Haugen, J., and Machenhauer, B.: A spectral limited-area formulation with time-dependent boundary conditions applied to the shallow-water equations. Mon. Wea. Rev., 121, 2618–2630, 1993.

[Hortal(2002)] Hortal, M.: The development and testing of a new two-time-level semi-Lagrangian scheme (SETTLS) in the ECMWF forecast model. Q.J.R. Meteorol. Soc., 128: 1671–1687, 2002.

[Horvath et al.(2011)] Horvath, K., Bajić, A., and Ivatek-Šahdan, S.: Dynamical downscaling of wind speed in complex terrain prone to bora-type flows, J. Appl. Meteor. Climatol., 50, 1676–1691, 2011.

[Horvath et al.(2009)] Horvath, K., Ivatek-Šahdan, S., Ivančan-Picek, B., and Grubišić, V.: Evolution and structure of two severe cyclonic bora events: contrast between the northern and southern Adriatic, Weather and forecasting, 24, 946–964, 2009.

[Horvath et al.(2008)] Horvath, K., Lin, Y.-H., and Ivancan-Picek, B.: Classification of cyclone tracks over the Apennines and the Adriatic Sea, Mon. Wea. Rev., 136, 2210–2227, 2008.

[Ivatek-Šahdan and Ivančan-Picek(2006)] Ivatek-Šahdan, S. and Ivančan-Picek, B.: Effects of different initial and boundary conditions in ALADIN/HR simulations during MAP IOPs, Meteorol. Z., 15, 187–197, 2006.

[Ivatek-Šahdan and Tudor(2004)] Ivatek-Šahdan, S., and Tudor, M.: Use of high-resolution dynamical adaptation in operational suite and research impact studies, Meteorol Z, 13(2), 1–10, 2004.

[Laprise(2003)] Laprise, R.: Resolved scales and nonlinear interactions in limited-area models, J. Atmos. Sci., 60, 768–779, 2003.

[Laprise(2008)] Laprise, R., de Elía, R., Caya, D., Biner, S., Lucas-Picher, P., Diaconescu, E., Leduc, M., Alexandru, A., Separovic, L., Canadian Network for Regional Climate Modelling and Diagnostics: Challenging some tenets of regional climate modelling. Meteorol. Atmos. Phys., 100, 3–22, 2008.

[Lionello et al.(2006)] Lionello, P., Bhend, J., Buzzi, A., Della-Marta, P. M., Krichak, S. O., Jansá, A., Maheras, P., Sanna, A., Trigo, I. F., and Trigo, R.: Cyclones in the Mediterranean region: climatology and effects on the environment, in: Mediterranean Climate Variability, edited by: Lionello, P., Malanotte-Rizzoli, P., and Boscolo, R., 325–372, Elsevier, 2006.

[Lynch and Huang(1992)] Lynch, P., and Huang, X-Y.: Initialization of the HIRLAM model using a digital filter. Mon. Wea. Rev, 120, 1019–1034, 1992.

[Lynch(1997)] Lynch, P.: The Dolph–Chebyshev Window: A Simple Optimal Filter. Mon. Wea. Rev., 125, 655–660, 1997.

[Lynch et al.(1997)] Lynch, P., Giard, D., and Ivanovici, V.: Improving the Efficiency of a Digital Filtering Scheme for Diabatic Initialization. Mon. Wea. Rev., 125, 1976–1982, 1997.

[Nicolis(2007)] Nicolis, C.: Dynamics of model error: The role of the boundary conditions. J. Atmos. Sci., 64, 204–215, 2007.

[Nutter et al.(2004)] Nutter, P., Stensrud, D., and Xue, M.: Effects of coarsely resolved and temporally interpolated lateral boundary conditions on the dispersion of limited-area ensemble forecasts. Mon. Wea. Rev., 132, 2358–2377, 2004.

[Rádnoti (1995)] Rádnoti, G.: Comments on A spectral limited-area formulation with time-dependent boundary conditions applied to the shallow-water equations. Mon. Wea. Rev., 123, 3122–3123, 1995.

[Robert(1982)] Robert A. 1982. A semi-Lagrangian and semi-implicit numerical integration scheme for the primitive equations. J. Meteor. Soc. Japan. 60 : 319 - 325.

[Simmons and Burridge (1981)] Simmons, A.J., and Burridge, D.M.: An Energy and Angular-Momentum Conserving Vertical Finite-Difference Scheme and Hybrid Vertical Coordinates. Mon. Wea. Rev. 109, 758–766, 1981.

[Stanešić(2011)] Stanešić, A.: Assimilation system at DHMZ: development and first verification results. Cro. Met. Jour., 44/45, 3–17, 2011.

[Staniforth(1997)] Staniforth, A.: Regional modelling: A theoretical discussion. Meteorol. Atmos. Phys., 63, 15-29, 1997.

[Termonia(2003)] Termonia, P.: Monitoring and improving the temporal interpolation of lateral-boundary coupling data for limited area models. Mon. Wea. Rev., 131, 2450–2463, 2003.

[Termonia(2004)] Termonia, P.: Monitoring of the coupling update frequency of a limited-area model by means of a recursive digital filter. Mon. Wea. Rev., 132, 2130–2141, 2004.

[Termonia(2008)] Termonia, P.: Scale-selective digital filter initialization. Mon. Wea. Rev., 136, 5246–5255, 2008.

[Termonia et al.(2009)] Termonia, P., Deckmyn, A., and Hamdi, R.: Study of the lateral boundary condition temporal resolution problem and a proposed solution by means of boundary error restarts. Mon. Wea. Rev., 137, 3551–3566, 2009.

[Termonia et al.(2011)] Termonia, P., Degrauwe, D., and Hamdi, R.: Improving the Temporal Resolution Problem by Localized Gridpoint Nudging in Regional Weather and Climate Models. Mon. Wea. Rev., 139, 1292–1304, 2011.

[Termonia et al.(2012)] Termonia, P., Voitus, F., Degrauwe, D., Caluwaerts, S., and Hamdi, R.: Application of Boyds Periodization and Relaxation Method in a Spectral Atmospheric Limited-Area Model. Part I: Implementation and Reproducibility Tests. Mon. Wea. Rev., 140, 3137–3148, 2012. doi: http://dx.doi.org/10.1175/MWR-D-12-00033.1

[Tudor and Ivatek-Šahdan(2010)] Tudor, M., and Ivatek-Šahdan, S.: The case study of bura of 1^{st} and 3^{rd} February 2007, Meteorol. Z., 19(5), 453–466, 2010.

[Tudor et al. (2013)] Tudor, M., Ivatek-Šahdan, S., Stanešić, A., Horvath, K., Bajić, A.: Forecasting Weather in Croatia Using ALADIN Numerical Weather Prediction Model. In: Climate Change and Regional/Local Responses. Eds: Zhang, Y. and P. Ray, InTech, Rijeka, 59–88, 2013.

[Tudor and Termonia(2010)] Tudor, M. and Termonia, P.: Alternative formulations for incorporating lateral boundary data into limited area models, Mon. Wea. Rev., 138, 2867–2882, 2010.

[Uppala et al.(2005)] Uppala, S. M., Kållberg, P. W., Simmons, A. J., Andrae, U., Bechtold, V. D. C., Fiorino, M., Gibson, J. K., Haseler, J., Hernandez, A., Kelly, G. A., Li, X., Onogi, K., Saarinen, S., Sokka, N., Allan, R. P., Andersson, E., Arpe, K., Balmaseda, M. A., Beljaars, A. C. M., Berg, L. V. D., Bidlot, J., Bormann, N., Caires, S., Chevallier, F., Dethof, A., Dragosavac, M., Fisher, M., Fuentes, M., Hagemann, S., Hólm, E., Hoskins, B. J., Isaksen, L., Janssen, P. A. E. M., Jenne, R., Mcnally, A. P., Mahfouf, J.-F., Morcrette, J.-J., Rayner, N. A., Saunders, R. W., Simon, P., Sterl, A., Trenberth, K. E., Untch, A., Vasiljevic, D., Viterbo, P. and Woollen, J.: The ERA-40 re-analysis. Q.J.R. Meteorol. Soc., 131: 2961–3012. doi: 10.1256/qj.04.176, 2005.

[Vánnitsem and Chome (2005)] Vánnitsem, S., and Chome, F.: One-way nested regional climate simulations and domain size. J. Climate, 18, 229–233, 2005.

[Warner et al.(1997)] Warner, T., Peterson, R., and Treadon, R.: A tutorial on lateral boundary conditions as a basic and potentially serious limitation to regional numerical weather prediction. Bull. Amer. Meteor. Soc., 78, 2599–2617, 1997.

[Wernli et al.(2002)] Wernli, H., Dirren, S., Liniger, M.A., and Zillig, M.: Dynamical aspects of the life cycle of the winter storm Lothar (24–26 December 1999). Q. J. R. Meteorol. Soc., 128, 405–429, 2002.

[Žagar et al.(2013)] Žagar, N., Honzak, L., Žabkar, R., Skok, G., Rakovec, J., and Ceglar, A.: Uncertainties in a regional climate model in the midlatitudes due to the nesting tecnique and the domain size, J. Geophys. Res. Atmos., 118, 6189–6199, 2013.